Vol. 11 No. 56 *Journal of the Radio Research Laboratories* *July 1964*
Printed in Tokyo, Japan pp. 197-250

UDC 550.377

SYNTHETIC STUDY OF SEVERE SOLAR-TERRESTRIAL DISTURBANCES ON FEBRUARY 9-12, 1958

By

Yukio HAKURA
The Radio Research Laboratories, Tokyo, Japan
and
Masao NAGAI
Magnetic Observatory, Kakioka, Ibaragi, Japan

(Received May 22, 1964)

Contents

Abstract 198
1. Introduction 198
2. General View of Solar-terrestrial Disturbances on Feb. 9-12, 1958 200
3. Detailed Discussions on Several Characteristic Phases of the Disturbances 208
 3.1. First impact of solar cosmic rays on the earth's polar ionosphere-onset of (PCA)p 208
 3.2. Sudden development of PCA in the auroral zone and associated polar magnetic disturbance far before the sudden commencement - $(PCA)_A$ and DP (PreSC) 212
 3.3. Unusual increase of ionization right before the SC 1 - (PCA) preSC 1... 217
 3.4. Outstanding geomagnetic and ionospheric disturbances associated with two successive sudden commencements - SCA 1 and SCA 2; DP (SC 1) and DP (SC 2) 219
 3.5. Remarkable deformation of PCBO region, and development of AZBO and storm E_s in the course of geomagnetic storm 224
 3.6. Two characteristic phases of $F2$-layer storm - D 1 ($F2$) and D 2 ($F2$) 226
4. Conclusions 230
Acknowledgments 232
References 232
Appendices
 I. Data used in the present paper 236
 II. Method of obtaining Dst and Ds variations of $f_0{}^*F2$, $h'{}^*F2$ and geomagnetic storm 243

III. SID effect of solar flare observed at 21: 08 on Feb. 9, 1958 245
IV. Additional world charts of $F2$ layer storm (prepared by Sawada and Hakura) 246

ABSTRACT

A comprehensive study is presented on the great solar-terrestrial disturbances on Feb. 9-12, 1958. The whole aspects of the disturbances have been examined mainly on the basis of statistical analysis of the world-wide ionospheric and geomagnetic data, with supplementary use of other solar-geophysical data such as flares, solar radio emissions, aurora and cosmic rays.

In the analysis, the first invasion of solar cosmic rays was detected as the outset of a slight ionospheric PCA near the geomagnetic poles after considerably long delay from a major flare that appeared at the centre of the solar disk at 21: 08 UT on Feb. 9. After the first occurrence of PCA, the enhanced ionization in the polar region underwent six-stepped transformations in the course of storm-time. They are understood in terms of the modulation process of solar cosmic rays due to the advancing solar magnetized gas cloud, shock front ahead of it, and ambient interplanetary magnetic fields as well as the transcient changes of the geo-magnetosphere at the attainment of the gas cloud to the earth.

There are several interesting aspects of the geomagnetic storm, such as the simultaneous occurrence of a peculiar polar disturbance with a PCA, two-stepped sharp sudden commencements, spectacular appearance of polar disturbances following the SC's, giant pulsations at the initial phase, and outstanding southward shift of current systems at the maximal phase of Dst-field. They occurred successively in close connexion with the appearance and the transition of ionospheric storms, aurora, and cosmic ray storms.

In the pulsating phase of geomagnetic storm, an unusual expansion of $F2$ layer was observed all over the world. Heating of upper atomosphere due to successive invasion of HM-wave is considered to be an origin.

1. Introduction

During the last period of high sunspot activity, a number of outstanding terrestrial disturbances were observed in association with the occurrences of major solar flares. These observational data afford an excellent test material of clarifying the nature of the charged corpuscles emitted from the sun, their propagation mechanism through the interplanetary space, and their interaction modes with the earth's upper atmosphere.

Among them, the solar-terrestrial disturbances on Feb. 9-12, 1958, is known as one of the severest ever recorded. Thus, in various fields deep interest has been concentrated on this event, and until now a large number of research papers have been published in discussion about many interesting aspects of the disturbance (for example, Akasofu and Chapman, 1962; Axford and Reid, 1962 and 1963; Blokh, et al., 1961; Fukushima and Abe, 1958; Hakura and Takenoshita, 1958; Hakura, et al., 1958; Hakura, 1961-b; Hikosaka, 1958; Huruhata, 1958; Kondo, et al., 1959; Leinbach, 1962; Matuura, 1963; Nagai, 1964; Nakata, 1958;

Obayashi, 1958; Obayashi and Hakura, 1960-a and -b; Piddington, 1963; Sakurai, 1961; Sato, 1959; Sinno, 1958, 1961; Somayajulu, 1963; Winckler, et al., 1959; Yonezawa, 1962).

In the earlier papers, we already clarified several important characteristics of the event, especially in the field of solar cosmic ray effect on the earth's polar ionosphere. The existence of PCA (Polar Cap Absorption) was first detected on the world-wide analysis of ionospheric sounding data (Hakura, et al., 1958). The importance of solar radio outbursts of type IV for occurrence of PCA was recognized through a statistical examination of solar-geophysical data (Hakura and Goh, 1959). On the general theory of the earth storm, the progressive patterns of PCA event were explained from somewhat wider view of the solar-terrestrial relationship (Obayashi and Hakura, 1960-a and -b).

However, the research papers in other fields have revealed more and more complicated features of the events. New facts thus clarified urge us to do further research in the detailed structure of the disturbances. In the present paper, an attempt is made to reexamine the whole aspects of February 1958 event on the analysis of ionospheric and geomagnetic data with supplementry use of other solar-geophysical observations such as flares, solar radio emissions, cosmic rays and aurora, in order to obtain the general morphology of the great solar-terrestrial disturbances.

To start with, a precise description of the disturbances is given in the following section, where will be outlined the whole course of February 1958 event and defined various distinct stages that compose the present earth storm. In the six subsections, several interesting phases of the disturbance are described and discussed in detail. The first is of the initial phase of the PCA event which concerns the problem of the first impact of solar cosmic rays on the earth's polar ionosphere. Special attention was paied confirming the existence of PCA with long delay upon which several authors have thrown doubts from a theoretical point of view. The development of impact zone is further discussed in the second subsection on examinations of progressive pattern of the PCA region. At this stage, a sudden development of PCA occurred in the auroral zone, in association with a peculiar type of polar magnetic disturbance. The third subsection deals with an unusual increase of PCA right before the sudden commencement which was originally discussed by Axford and Reid (1962). Immediately after two successive sudden commencements of the geomagnetic storm, the entire world was covered by severe disturbances of the polar origin. The fourth subsection treats the problem in view of the simultaneous boundary changes of the events, concerned with the distortion of the earth's magnetosphere at the attainment of shock waves responsible for the SC's. Soon after the second SC, the region of PCA underwent remarkable deformation, as the storm-type sporadic E layer appeared over the polar ionosphere. The marked transformation of the ionospheric disturbances in the course of the geomagnetic storm is the main subject in the fifth subsection. During the initial phase of the geomagnetic storm which is characterized by its giant pulsations, an unusual expansion of the $F2$ layer was observed all over the world. This is our final topic to be treated in the sixth subsection.

2. General View of Solar-terrestrial Disturbances on Feb. 9–12, 1958

Table 1 gives the whole scheme of solar-terrestrial disturbances on February 9–12, 1958. It is summarized in twelve characteristic stages which are nominated, for convenience, $\sum$, α, β, ..., and λ. Before entering into detailed discussion of these characteristic phases, we shall present here some introductory descriptions of the solar-terrestrial disturbances.

A solar flare responsible for the disturbances (stage $\sum$)

The solar event that gave rise to the disturbances has been identified as a flare of importance 2+ that appeared at 21: 08 UT on Feb. 9, because the simultaneous occurrence of type IV outbursts (see Fig. 1-(A)) strongly supported the

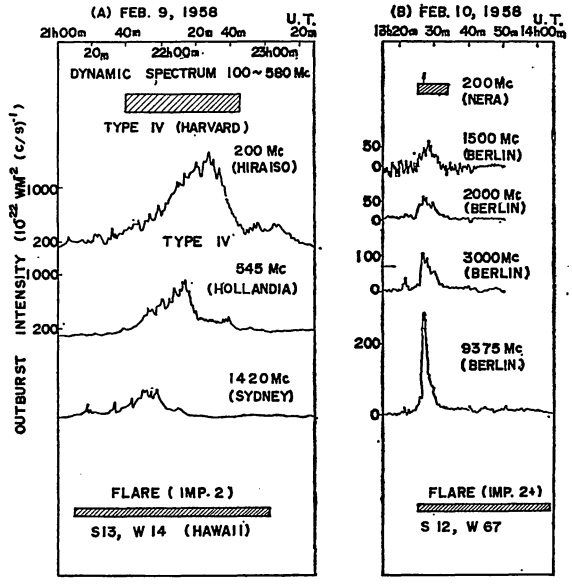

Fig. 1. Two major outbursts which preceded the terrestrial disturbance on Feb. 10–12, 1958.
(A) Outbursts at 21: 08 on Feb. 9: this flare is identified as an origin of the successive terrestrial disturbances discussed in the present paper.
(B) Outbursts at 13: 25 on Feb. 10.

production of the solar cosmic rays which induced the terrestrial PCA event after some delay from the flare (Hakura and Goh, 1959; Obayashi and Hakura, 1960-a). Though some authors suggested the storm-producing possibility of the flare of importance 2+ that was observed at 13: 25 UT on Feb. 10 (see Fig. 1-(B)), it is not the case, since its starting time was 8 hours behind the onset of (PCA)p event as descrivbed later. Even in case of a solar cosmic ray flare, it would act only to give variety to the mode of PCA pattern, through an interaction with the foregoing corpuscular cloud emitted from the sun at the time of the former flare.

Table 1 Scheme of Solar-ter

Stage		Σ	α	β	γ	δ
Time (U. T.)		9th 21 : 08	10th 05～07→	12→	11th 00 : 15*→	01 : 26
Solar Events		Flare (Imp. 2+) (S 13, W 14) Type IV OB				
Ionospheric Storms	Absorption	SID (Pre-existing AZA)	$(PCA)_P$ starts at solar side polar region.	$(PCA)_A$ starts at solar side auroral zone.	$(PCA)_{Pre\ SC1}$ starts. (Axford-Reid)	SCA1 + $(PCA)_{Pre\ SC2}$
	D(E_s)	(Pre-existing *Es*)				
	D($F2$)			← Enhanced f_oF2 at polar regio		
	Aurora					01 : 30——
Geomagnetic Storm		Slight perturbation	Dead calm	← DP (Pre SC) →		SC1, DP (SC_1)
C. R. Storm						Dst starts. (01h)
Remarks			τ_p=8h～10h	τ_A=15h	*after 00 : 00 WPCBO	ΔT_m=28h

SID

During the solar flare of stage∑, a slight SID (Sudden Ionospheric Disturbance) was observed over the whole sunlit hemisphere; this event is due to the ionizing effect of solar X-rays which penetrate into the ionosphere and are absorbed at its *D*-region. Detailed discussion of the SID is given in Appendix III.

PCA's and the following earth storms

After some delay-time from the SID, solar cosmic rays attained to the earth and began to impinge upon its polar ionosphere, producing a series of PCA events. A great geomagnetic storm of SC type occurred at 01: 26 on Feb. 11 (see Fig. 2). This was on unusually large scale and accompanied with a cosmic ray

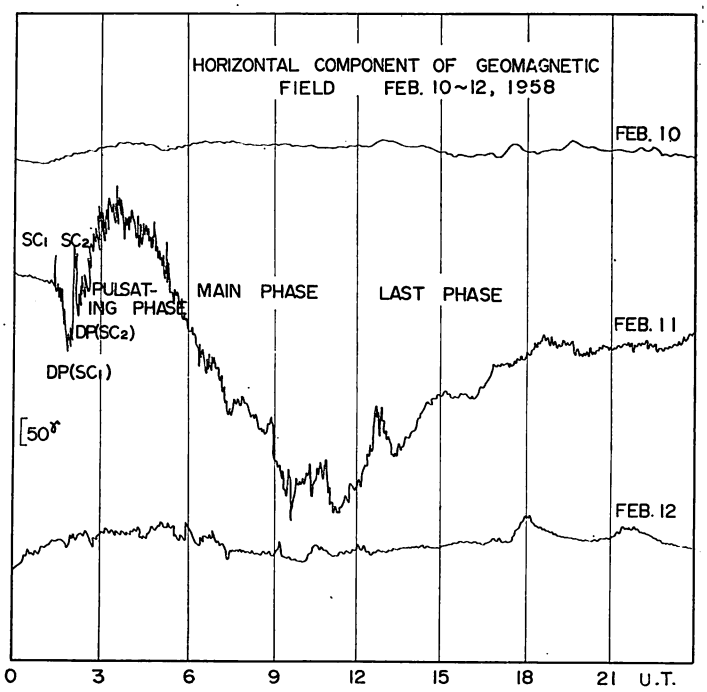

Feb. 2. Horizontal component of geomagnetic field intensity on Feb. 10-12, 1958, observed at Kakioka, Japan.

storm, intense aurora, polar blackouts, storm E_s, and $F2$-layer disturbances of peculiar feature.

Figs. 3-(1)~(16) show a series of synoptic patterns of blackouts (contours of Δf_{min}: hatched regions), storm E_s (contours of f_oE_s: dotted regions), and $F2$-layer storms (contours of f_o*$F2$), drawn on the map viewed from the northern geomagnetic pole, with the patterns of equivalent current system which are responsible for the Ds-field of geomagnetic disturbances. The source of data and the method of analysis are explained in Appendix I. By consultion with the nomi-

estrial Disturbances on Feb- 9—12, 1958

ε	ζ	η	θ	ι	κ	λ
01 : 59	02 : 30	03 : 00→	06→	10∼11	∼13	12th 14
SCA2	Deformed B. O. Region {Reduced PCA {Developed AZA}			MAX : AZA Equatorward Shift		
		Storm E_s observed				
→	← D1($F2$) →		D2($F2$) →		Max. of D2($F2$)	Last of D2($F2$)
	→03 : 30		←	intense aurora observed in Japan →		
very intense diffuse green arc 02 : 00 (Max.) red color intense aurora						
SC2, DP (SC_2)		Main Phase starts.	Main Phase	Max. Stage ΔH_K=617 γ*		
	← pulsating →					
				Ist		
				*at Kakioka		

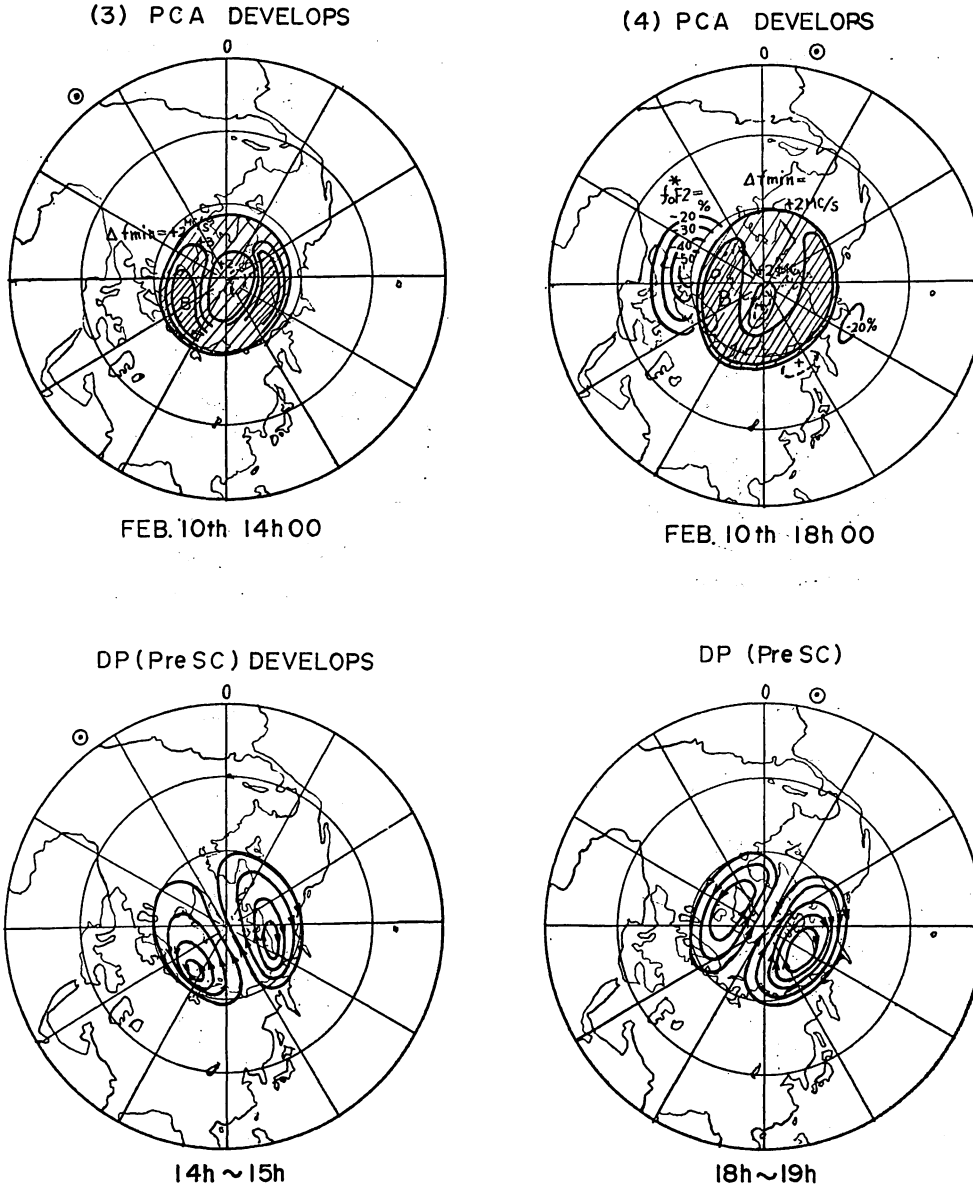

geomagnetic storms on Feb. 10–12, 1958, drawn on the northern world maps

f min (hatched).
ed by thick hatches.
ed by dots.
deviation of critical frequency (f_0*$F2$).

alent current system,
s 1×10^5 amp.

(5) DEVELOPMENT OF PCBO

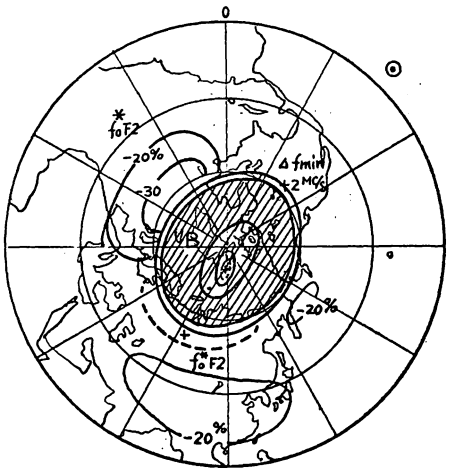

FEB. 10th 20h 00

(6) Pre SC1
WPCBO (WHOLE POLAR CAP B.O.)
(PCA) PreSC1
ENHANCED foF2 AT POLAR REGION

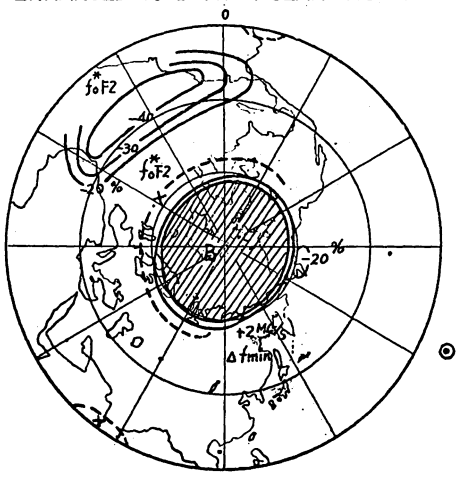

FEB. 11th 01h 00 (-25min)

DP (Pre SC)

20h ~ 21h

DP (Pre SC)

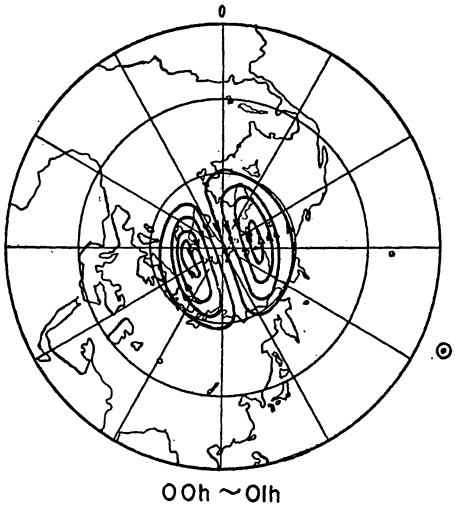

00h ~ 01h

(7) AFTER SC1
ENLARGED WPCBO
SC1

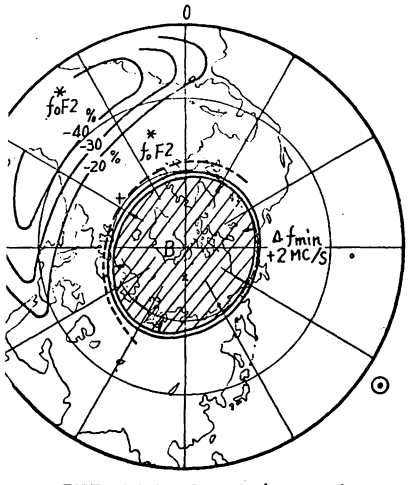

FEB. 11th 01h 30(+5min)
01h 45(+20min)

(8) AFTER SC2
FURTHER ENLARGED WPCBO
SCA2

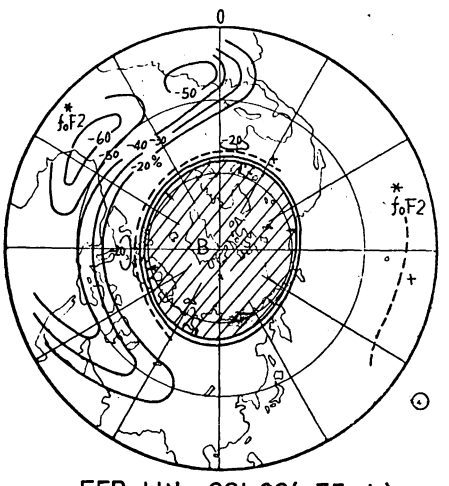

FEB. 11th 02h 00(+35min)
02h 15(+50min)

DP (SC1)

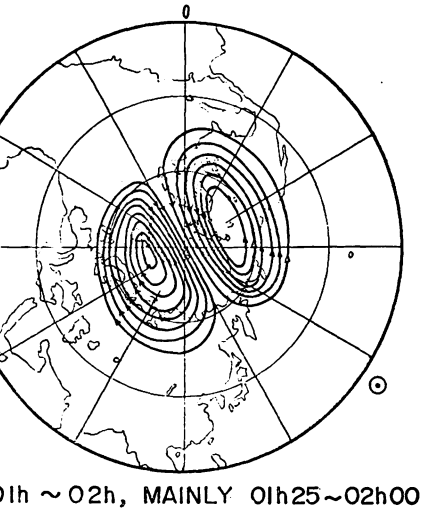

01h ~ 02h, MAINLY 01h25~02h00

DP (SC2)

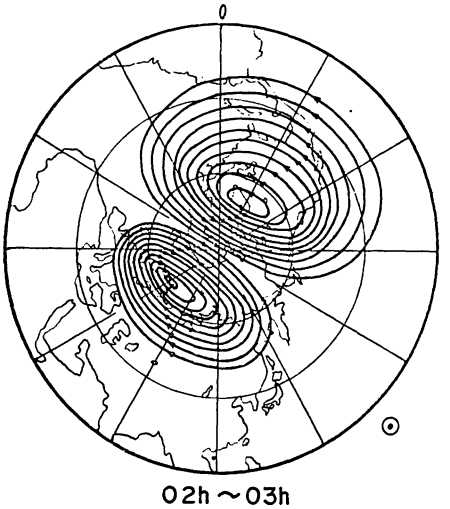

02h ~ 03h

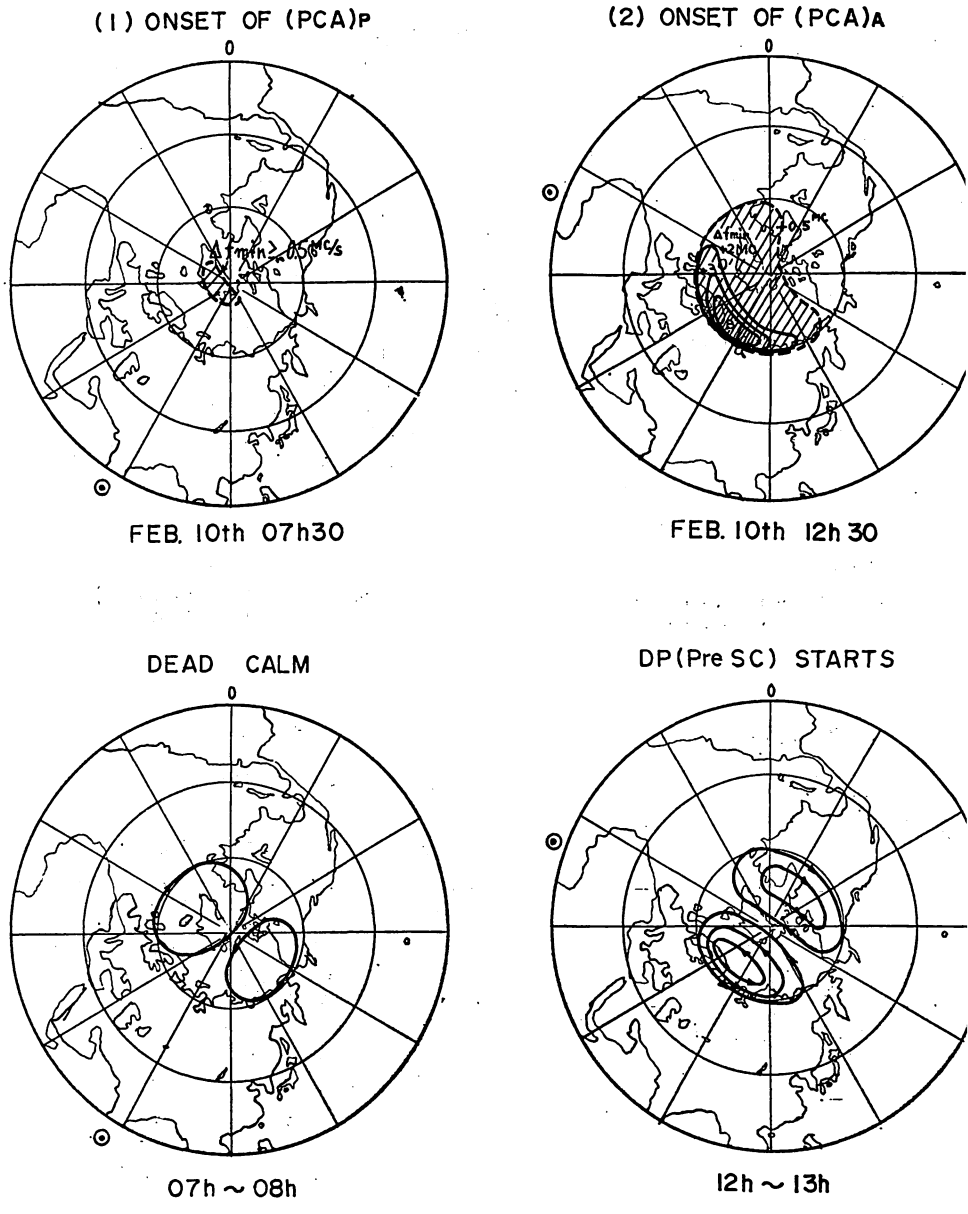

Fig. 3-(1)~(16) Sixteen characteristic stages of ionospheric and
in geomagnetic coordinates.

Ionospheric storms (upper figures):

Enhanced ionization is expressed by the contour of
The region of complete polar blackouts (B) is indica
The region where $f_0E_s \geq 5$ Mc/s (storm *Es*) is indica
The *F*2 layer storm is expressed by the percentage
(decrease: continuous line; increase: broken line)

Geomagnetic storm (lower figures):

Ds-field of geomagnetic storm is expressed by equiv
where the electric current between successive lines

(11) AZBO & STORM Es
REDUCED D1(F2)

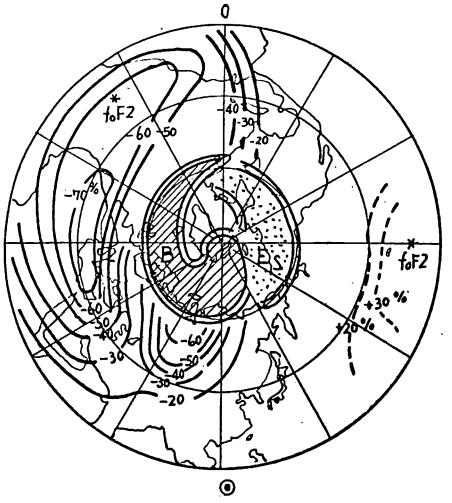

FEB. 11th 05h00

MAIN PHASE (PULSATING)

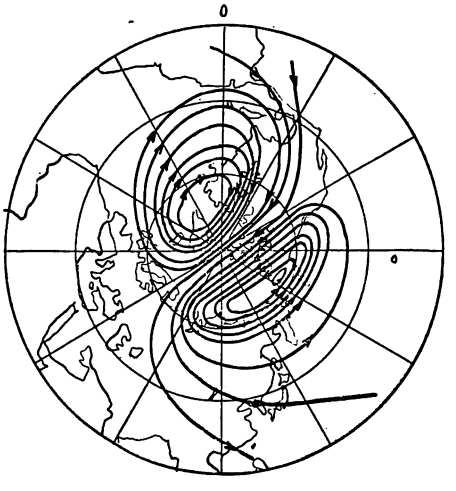

⊙ 05h~06h

(12) AZBO & STORM Es
D2(F2) AT HIGH LATITUDE

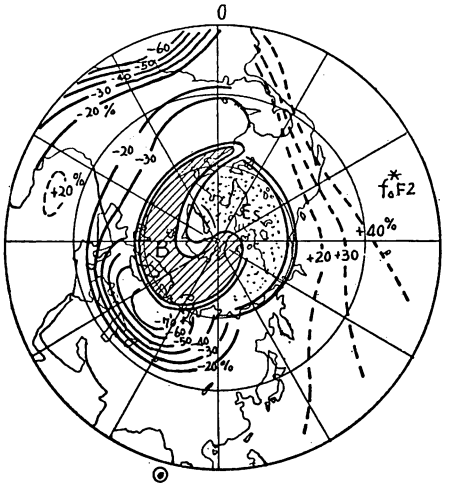

FEB. 11th 06h00

MAIN PHASE

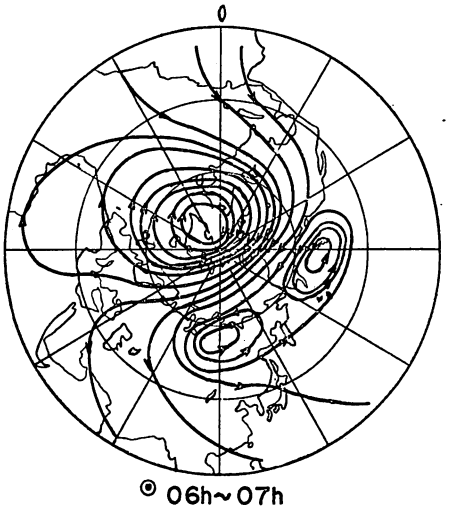

⊙ 06h~07h

(13) DEVELOPED D_2(F2)

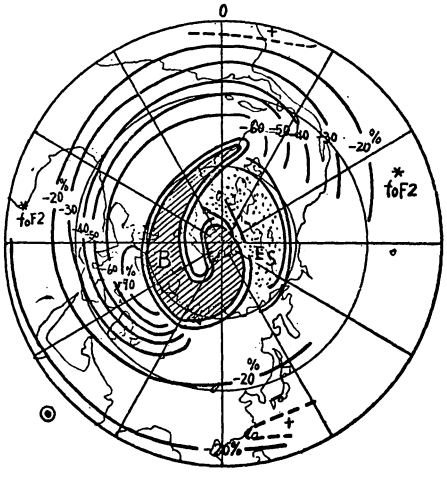

FEB. 11th 08h00

MAIN PHASE

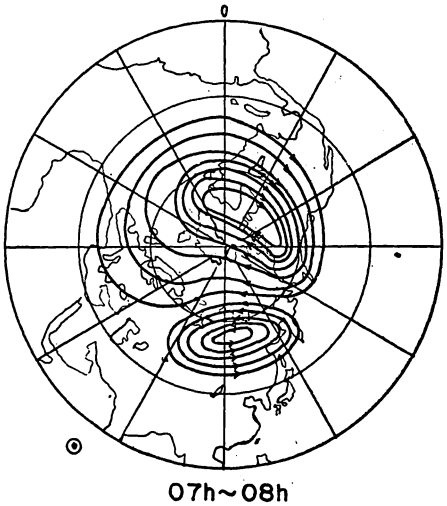

07h~08h

(14) MAX. OF Dst (MAGNE. STORM)
EQUATOR-WARD SHIFT OF
AZBO DEVELOPED D_2(F2)

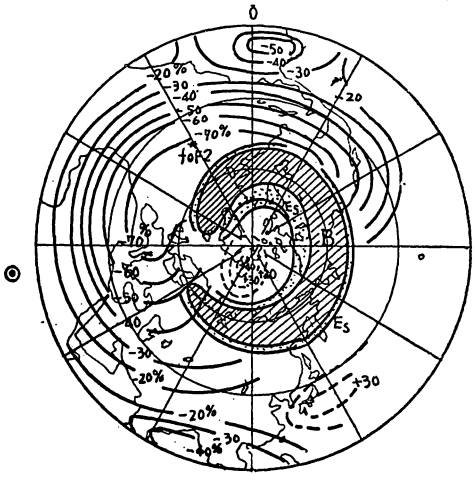

FEB. 11th 10h30, 11h00

MAIN PHASE

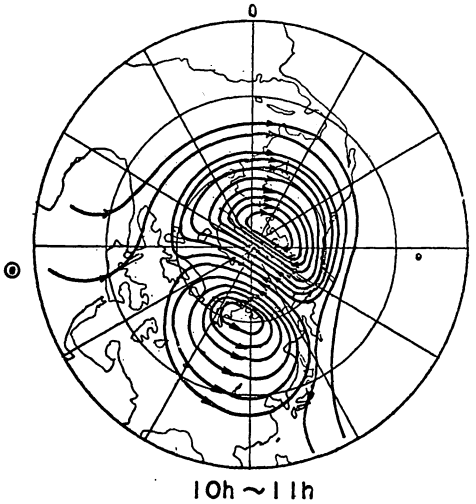

10h ~ 11h

(15) SURVIVING D_2(F2)

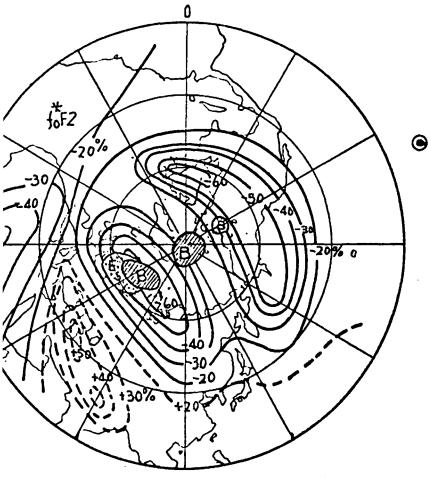

FEB. 11th 22h00

(16) LAST PHASE OF D_2(F2)

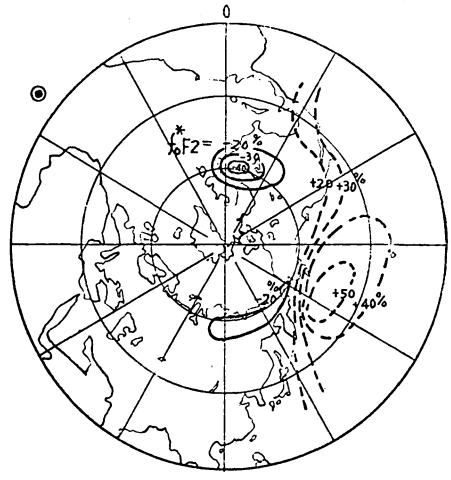

FEB. 12th 13h00, 14h00

LAST PHASE

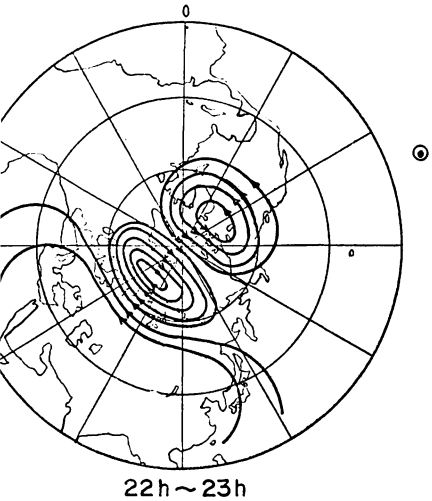

22h~23h

LAST PHASE

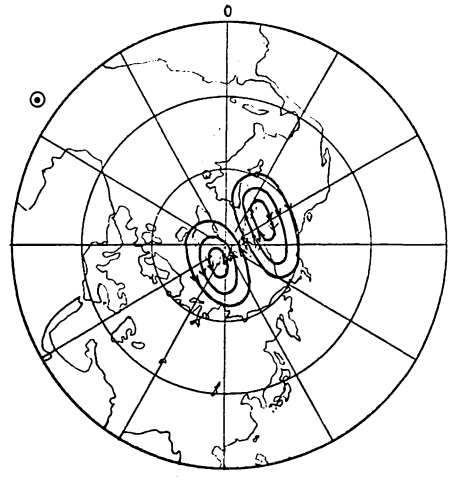

13h~14h

(9) DEFORMED B.O. REGION
STORM Es
UNUSUAL F2 LAYER STORM: DI(F2)

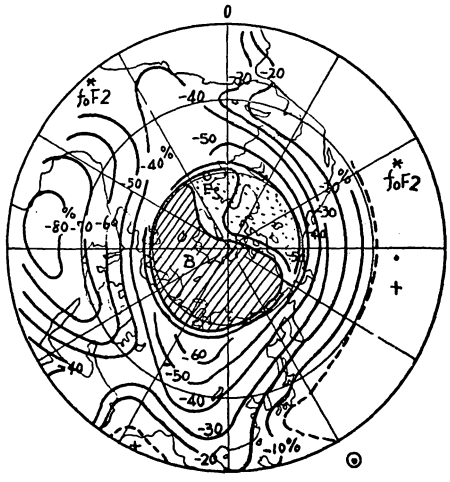

FEB. 11th 03h00 (+95min)

MAIN PHASE (PULSATING)

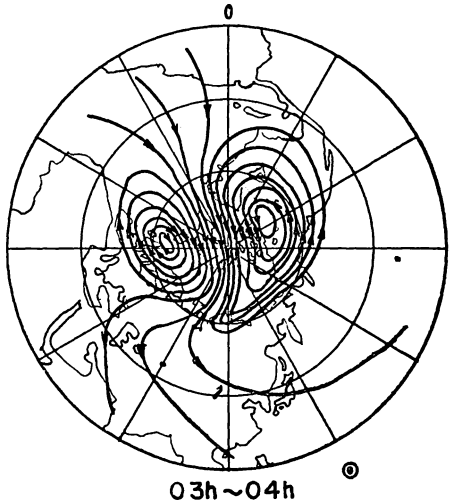

03h~04h

(10) AZBO & STORM Es
DI(F2) MAX.

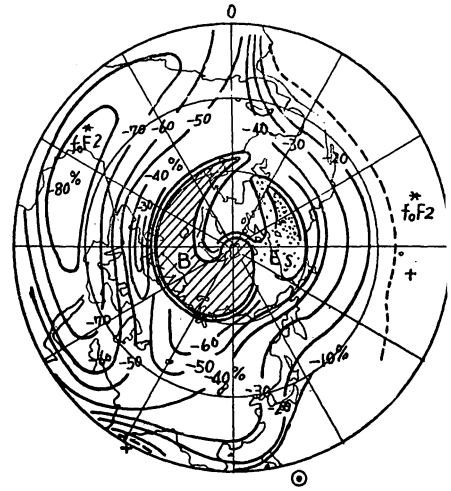

FEB. 11th 04h00

MAIN PHASE (PULSATING)

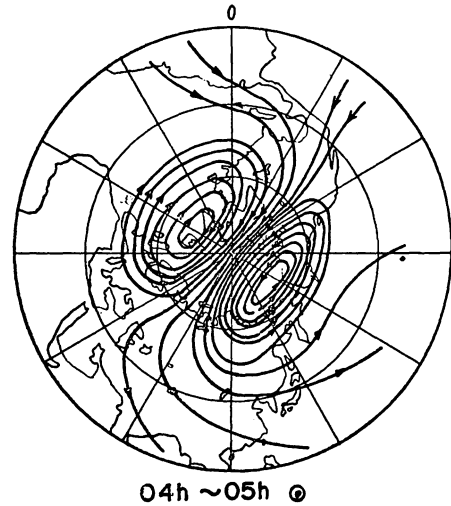

04h ~05h

nations given in Table I, the terrestrial disturbances are outlined as follows:
(1) A slightly ionized region ((PCA)p) appeared on the solar side of the polar region at 07 h UT on Feb. 10, when the geomagnetic condition was deadly calm. This seems to be the first impact of solar cosmic rays on the earth's polar ionosphere.....(stage α)
(2) At about 12 h on Feb. 10, the PCA event showed a sudden development on the sunlit side of the auroral zone ($(PCA)_A$). Simultaneously, a current system of polar geomagnetic disturbance (DP(PreSC)) was formed, originating in the region of increased ionization. It should be noted that the polar geomagnetic disturbance started far before the sudden commencement at 01: 26 on Feb. 11. .....(stage β)
(3)~(5) The region of $(PCA)_A$ was elongated to the night side, and the whole auroral zone was covered by complete blackouts within several hours, while the ionization was gradually intensified in the polar region.
(6) Right before the sudden commencement, i.e. at 01: 00 on Feb. 11, the whole polar cap suffered from complete blackouts (WPCBO). At this stage, an unusual increase of ionization was detected by the cosmic noise absorption measurement (Axford and Reid, 1962). .....(stage γ)
(7) As shown in Fig. 2, two sharp sudden commencements occurred successively, first at 01: 26 (SC1) and then at 01: 59 (SC2) on Feb. 11, both of which were followed by severe polar disturbances DP (SC1) and DP (SC2). A remarkable pulsation was observed during the initial phase of the geomagnetic storm.

At the time of SC 1, the region of PCBO showed considerable enlargement due to the occurrence of SCA 1, a kind of "sudden commencement absorption." A wide-spread current system of polar origin gives the Ds-field of DP (SC 1). .....(stage δ)
(8) At the SC 2, the region of PCBO is enlarged further down to unexpectedly low latitude zone. This is attributed to the occurrence of SCA2. The corresponding current system (DP(SC2)) also showed a remarkable expansion to cover almost the entire world. .....(stage ε)
(9)~(11) From 02: 30 to 05: 00, the geomagnetic storm showed quite a pulsating feature. During these intervals, the region of blackouts experienced a considerable deformation, that is, on the evening side, the region of PCA quickly retired up to the north pole, while, on the morning side, it deformed itself into some spiral pattern. This is the onset of Auroral Zone Blackout (AZBO). At the same time, the region of storm E_s developed on the evening side, embraced with the pattern of AZBO. At this phase of disturbance, an outstanding depression of f_oF2 suddenly covered the whole world. The depression was especially severe on the morning side of lower latitude zones. This is a peculiar type of $F2$-layer storm, and named D1($F2$) to distinguish it from the usual type of $F2$-layer storm (D2($F2$)) which appeared at a later stage. .....(stage ζ, η)
(12)~(13) After 06 h on Feb. 11, the ionospheric disturbances showed characteristics quite similar to those at the event on Sept. 13, 1957, which were already discussed elsewhere, (Hakura, Nagai, and Sano, 1961). The region of auroral zone blackouts formed a spiral-like pattern over the morning hemisphere, embraced with the region of storm E_s which extended on the evening side. The outer edges of the disturbed region showed gradual equatorward shifting, in coincidence with the development of auroral zone currents of the Ds field. In these stages, the ordinary

$F2$-layer storm (D2($F2$)) started in the sunlit auroral zone and gradually enlarged its region along AZBO. .....(stage θ)

(14) At the maximal phase of the Dst-field (at 10h–11h on Feb. 11), the pattern of polar blackouts and storm E_s showed considerable equatorward shifting, as the deterioration of f_0F2 developed to cover the whole world. .....(stage ι)

(15)~(16) During the last phase of the geomagnetic storm, the ionospheric disturbance gradually decayed till it was entirely recovered earlier at 13h-14h on Feb. 12. This is the end of our severe solar-terrestrial disturbances. .....(stage λ)

3. Detailed Discussions on Several Characteristic Phases of the Disturbances

3.1. First impact of solar cosmic rays on the earth's polar ionosphere - onset of (PCA)p.

At the outset, we shall choose a topic of the first impact of solar cosmic rays into the earth's polar ionosphere. The problem here is to examine when and where the polar cap absorption started after the occurrence of cosmic ray-producing flare at 21 : 08 on Feb. 9.

In Fig. 4, the first possible onset times of PCA at northern and southern polar

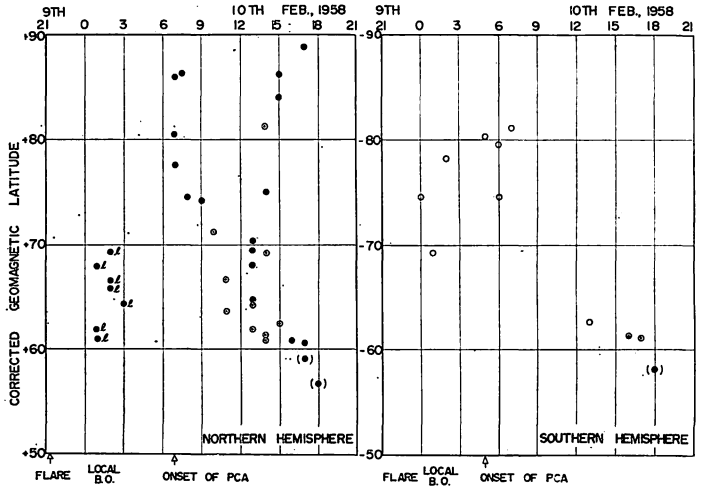

Fig. 4. Time of the first possible onset of PCA in the order of corrected geomagnetic latitudes.

○ : Sunlit during 00^h~12^h

◉ : Sunlit at the time of PCA-start

● : Dark at the time of PCA-start

( ) : Absorption of short duration

l : Local blackouts

stations are plotted in the order of corrected geomagnetic latitudes (for corrected latitudes, see Hakura 1964). The onset times are determined by the analysis of Δf_{min} for each station and thus their time accuracy is 15 minutes.

During 01h–03h on Feb. 10, some blackout conditions were observed at several northern auroral zone stations. However, these blackouts must be the remnants of the ionospheric disturbances which are associated with the foregoing s.s.c. at 13: 41 on Feb. 8, because there is no essential difference between two patterns of enhanced ionizations, when we compare the ionospheric condition at a pre-flare stage (Feb. 9, 21: 00) with that at 03: 00 on Feb. 10 (Fig. 5-1).

A systematic appearance of polar cap absorption was first seen after 07: 00 U.T. on Feb. 10 in the northern hemisphere, where the onset time is splitted into two groups. The first group started at 07: 00 around the northern pole and spread towards the auroral zone in 5 hours or so, whereas the second group commenced at 13: 00 in the auroral zone and the enhanced ionization gradually propagated to the polar region.

Fig. 5-2 shows the top-viewed patterns of the enhanced ionization in these initial phases of PCA, expressed by the contour map of Δf_{min}'s. At 07: 00, a slight but distinct increase of Δf_{min} was seen around the northern polar region on the solar side (the left figure). We shall call the enhanced ionization at the pole "(PCA)p-event" in the present paper, and this is the first impact of solar cosmic rays produced at the time of solar flare (21: 08 on Feb. 9). It should be noted that the pattern of (PCA)p was restricted first in a small region and thus showed a kind of impact zone. The enhanced ionization limited in the solar side is not the photo detachment effect due to the solar UV radiation, since the whole polar region is situated on the night side throughout the day during February.

As shown in Fig. 4, the region of (PCA)p was enlarged gradually toward the auroral zone until the occurrence of $(PCA)_A$, which will be discussed in the next subsection. Fig. 5-2-right shows an example of such an enlarged (PCA)p event right before the onset of $(PCA)_A$.

In the southern hemisphere, the absorption effects are much greater than in the northern hemisphere during this season. For instance, the (PCA)p in the southern hemisphere became detectable 2 hours earlier than in the northern hemisphere. However, the process of PCA development itself seems to be quite similar to that in the northern hemisphere.

Through these discussions, it is concluded that the PCA started at 05h–07h on Feb. 10 as a slightly enhanced ionization in some restricted area around the geomagnetic poles, and this is the first impact of solar cosmic rays which were produced at the time of great solar flare at 21: 08 on Feb. 9. This result provides a strict statistical reconfirmation of existence of slow occurrence type PCA event whose delay-time from the flare is far greater than the rectilinear travel time of solar cosmic rays through the interplanetary space (Sinno, 1961; Hakura, 1961-b, Obayashi, 1962; Leinbach, 1962). The delay-time of (PCA)p is 8 hours, whereas the traveling time of PCA-producing protons over a direct path is about an hour, since their energy is estimated of 10~100 MeV.

A possible explanation of such a long delay is the entrapment of solar cosmic rays in the magnetized solar plasma cloud, with subsequent release as the cloud expanded into the interplanetary space (Sinno, 1961). By some modification, this model could explain the characteristic features of (PCA)p-event.

As sketched in Fig. 6, an extended solar magnetic field is assumed to be convex

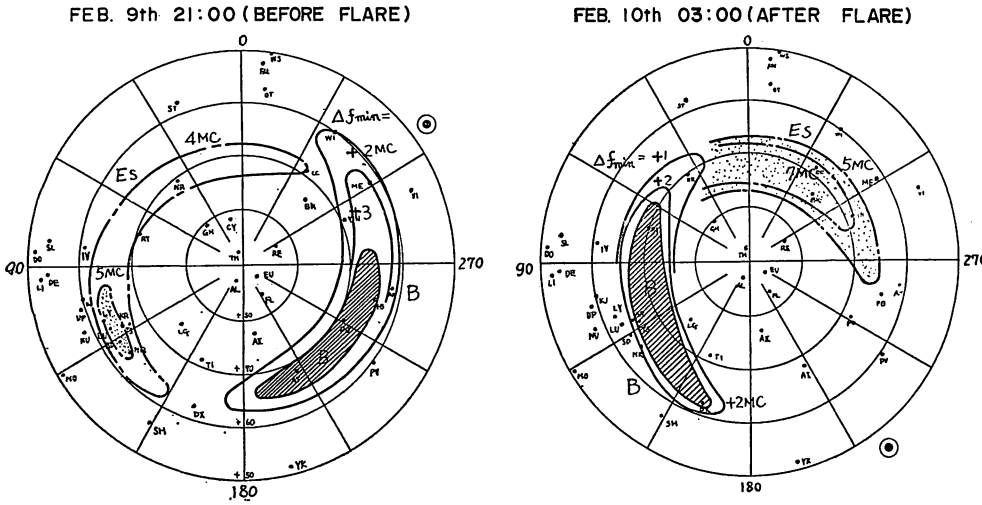

Fig. 5-1. Pre-existing auroral zone disturbances before and after the flare at 21:08 on Feb. 9, 1958 (northern geomagnetic coordinates).

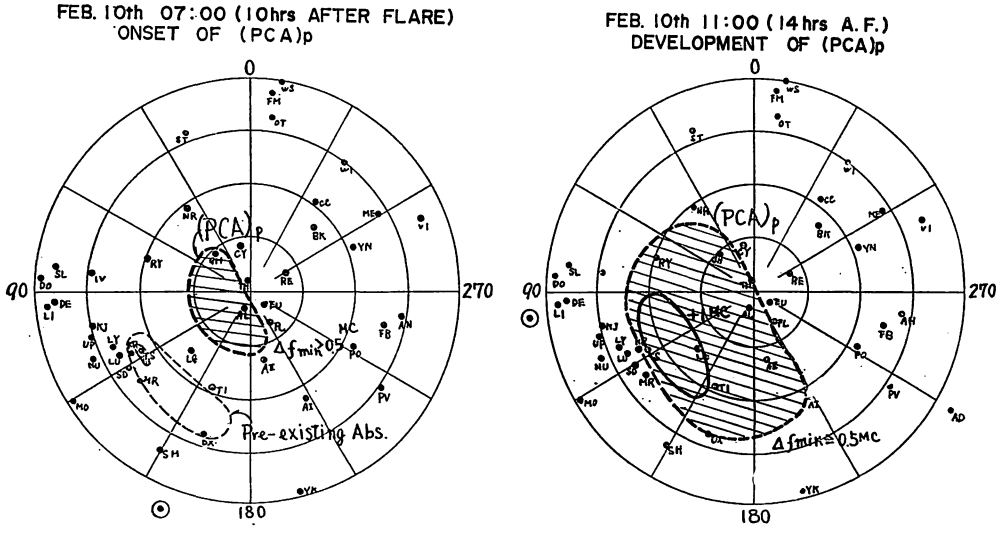

Feb. 5-2. Onset and development of (PCA)p (northern g.m. coordinates).

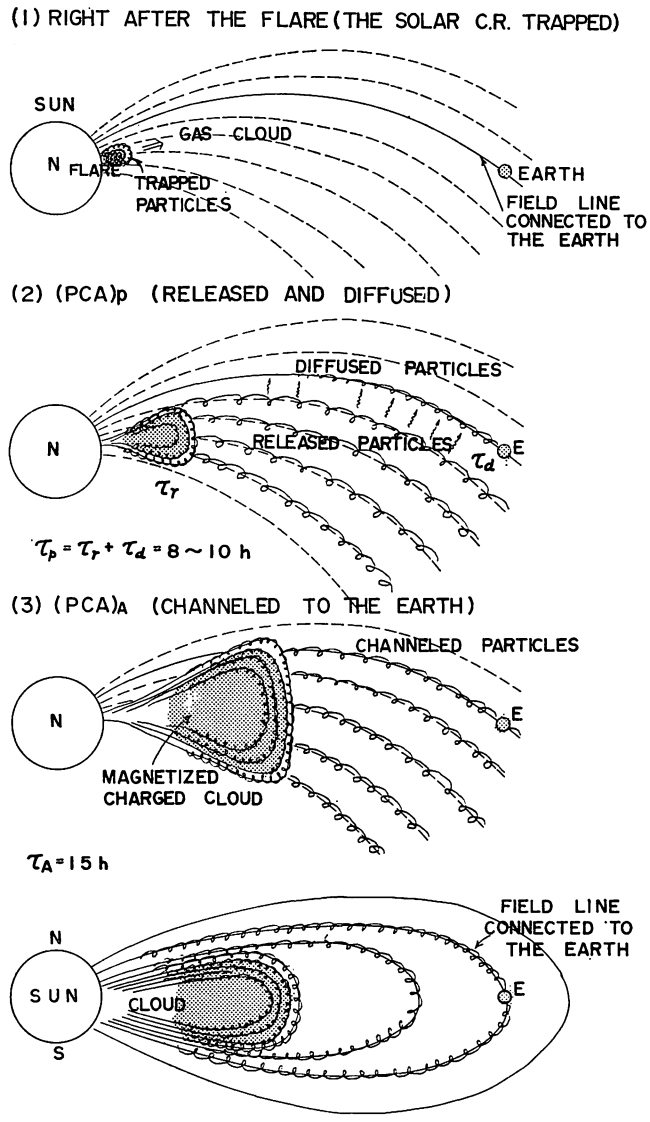

Fig. 6. Pictorial representations of a hypothetical mechanism which might explain the occurrence of (PCA)p and (PCA)A of long delay.

toward the west, and thus the magnetic field lines connected with the earth may emanate from somewhere on the western side of the solar disk as viewed from the earth, so that particles channeled to these field lines (indicated by continuous lines) can reach the earth with a short delay-time (Obayashi and Hakura, 1960-c). This is the basic structure of quiescent interplanetary space. Consider now the occurrence of a cosmic ray-producing flare in the central part of the solar disk. The ejected gas cloud carries out a part of sunspot magnetic fields into the inter-

planetary space. For a few hours, solar cosmic rays are kept inside the gas cloud trapped by these transported magnetic fields (stage (1) in Fig. 6). After some characteristic time (τ_r), the trapped particles begin to escape from the weakened magnetic field due to the outward expansion of the gas cloud. At the time of (PCA)p, the solar particles are supposed to be released into the magnetic field lines somewhat eastward from those connected to the earth (stage (2) in Fig. 6). Some diffusion mechanism due to magnetic field irregularities in the interplanetary space might convey the particles to the earth, so that the summation of release time (τ_r) with the diffusion time (τ_d) gives the delay (τ_p) of (PCA)p from the flare. The slight ionization (Δf_{min} was only 0.5 Mc/s till the onset of $(PCA)_A$) at the time of (PCA)p is thus understood in terms of such diffused solar cosmic rays.

As already mentioned, the initial pattern of (PCA)p is restricted in a polar region on the solar side. It is interesting to note that such impact region of solar cosmic rays includes the terminals of field lines connected to the vicinity of the magnetically neutral point on the cavity boundary which is formed by the interaction of the geomagnetic field with the ever-flowing solar wind. Through the neutral point, solar cosmic rays might easily enter the earth's atmosphere regardless of their energies (Akasofu, et al., 1963), so that the diffused solar cosmic rays, in spite of their low flux density, could produce the enhanced ionization around the effective pole which is situated in the polar region on the solar side, as calculated, for example, by Spreiter and Briggs (1962).

3.2 Sudden development of PCA in the auroral zone and associated polar magnetic disturbance far before the sudden commencement- $(PCA)_A$ and DP (PreSC)

In order to observe the development patterns of PCA from other point of view, Fig. 7 gives the storm-time change of $\overline{\Delta f_{min}}$ in the polar region (a) and in the auroral zone(b). Here, $\overline{\Delta f_{min}}$ means an average value of Δf_{min}'s at several selected stations, so that it gives a kind of Dst-variation of polar cap absorption. For comparison, it also gives the timely change of cosmic noise absorptions observed by riometers at two auroral zone stations, Fort Yukon (b') and Churchill (b'').

The thin line in the upper figure (a) is the $\overline{\Delta f_{min}}$ of 3 solar side stations and clearly shows the occurrence of (PCA)p event at 07h on Feb. 10 (indicated by the letter α). These curves of $\overline{\Delta f_{min}}$ in the polar region show a tendency of gradual increase of PCA till the occurrence of s.s.c.; it supports Sinno's argument (1961) for the existence of gradual type PCA. Leinbach (1962) classified such type of PCA as SC-max-extreme in his system.

On the other hand, the mean $\overline{\Delta f_{min}}$ at 7 auroral zone stations (b) shows a sudden increase of ionization at about 12 h on Feb. 10 (indicated by the letter β). The increase occurred in good time-coincidence with the distinct start of PCA at the riometer records of two auroral zone stations. This phase of PCA is named $(PCA)_A$ in the present analysis.

A series of spnoptic maps of Δf_{min} in Figs. 5-3 to-5 show the detailed progressive patterns of $(PCA)_A$ in the northern hemisphere. At 12: 00 on Feb. 10 (Fig. 5-3 left), the ionization suddenly started to increase over the sunlit auroral zone (around Tromsö). The region of abnormal ionization began to expand after 12: 30 (Fig. 5-3 right), and at 13: 00 (Fig. 5-4 left) it attained to the night side of the auroral zone

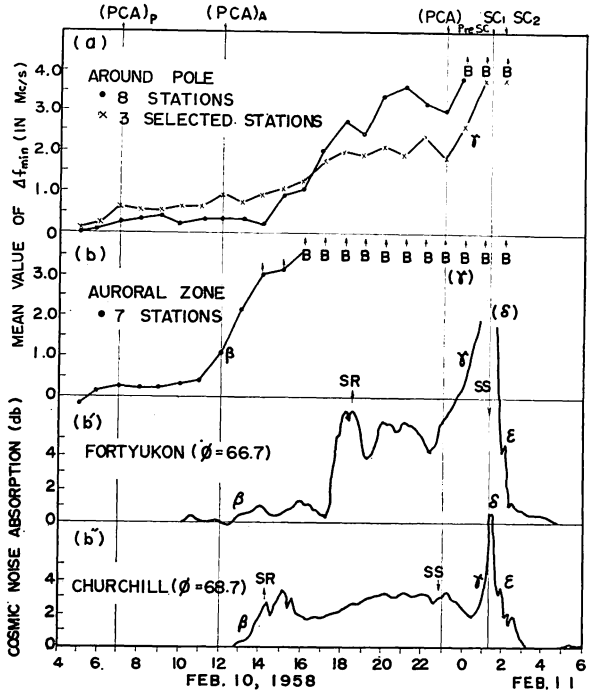

Fig. 7. Development of PCA around the pole (a) and in the auroral zone (b, b′, b″).
(a) Mean value of Δf_{min} at 8 polar stations: Thule, Eureka, Alert, Fletchers. Ice, Resolute Bay, Clyde River, Godhavn, and Arctic II (thick line).
×: Mean value of Δf_{min} at 3 stations of solar side: Alert, Godhavn, and Arctic II (thin line).
(b) Mean value of Δf_{min} at 7 statians: Tromsö, Dixon Is., Arctic I, Point Barrow, Churchill, Narsarssuak, and Reykjavik.
(b′), (b″) Cosmic noise absorption at Fort Yukon (27.6 Mc/s) and Churchill (30.0 Mc/s). (after Axford and Reid, 1962). SR: sunrise, SS: sunset.

including Fort Yukon and Churchill, where, at the same time, riometer records indicated a clear onset of cosmic noise absorption (see Fig. 7). The ionization continued to increase till the blackout condition covered the entire auroral zone earlier at 22: 00, whereas rather gradual increase was observed at the polar stations as shown in Figs. 5-4 and-5.

The development patterns of (PCA)A mentioned above would display the process of solar particle invasion into the polar ionosphere, even though the influence of solar UV radiation must be taken into account for the rate of ionization in the sunlit hemisphere. They describe the formation and growth of impact zone for the high energetic particles which produce the polar cap absorption. The sudden increase in number of invading particles at 12: 00 could be understood in terms of the achieved channeling of solar cosmic rays to the magnetic field lines which were connected to the earth. Propagating along these line of force, numerous solar cosmic rays could attain to the earth in a short times of delay. The situation is explained by a pictorial expression of Fig. 6-(3).

Another important characteristic of (PCA)A is the simultaneous occurrence of a severe polar geomagnetic disturbance which preceded the onset of s.s.c. on Feb. 11, 1958 (Nagai, 1964). Fig. 8 shows the storm-time variations of (a) $D_{st}^{32.5}$ and (b) ΔX_m of a geomagnetic storm (see Appendix II), in comparison with that of (c) cosmic noise absorption record at Fort Churchill. As indicated by the arrows in the figure, the pre-SC polar disturbance (DP (PreSC)) started at −13h of the storm time, showing rather surprising time-coincidence with the onset of (PCA)A. For

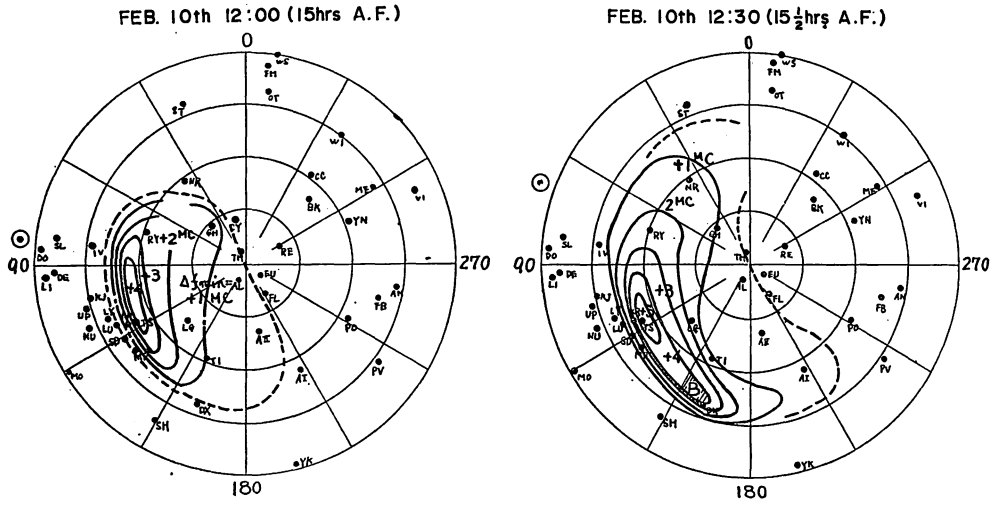

Fig. 5-3. Sudden development of PCBO: Onset of $(PCA)_A$ (northern g.m. coordinates).

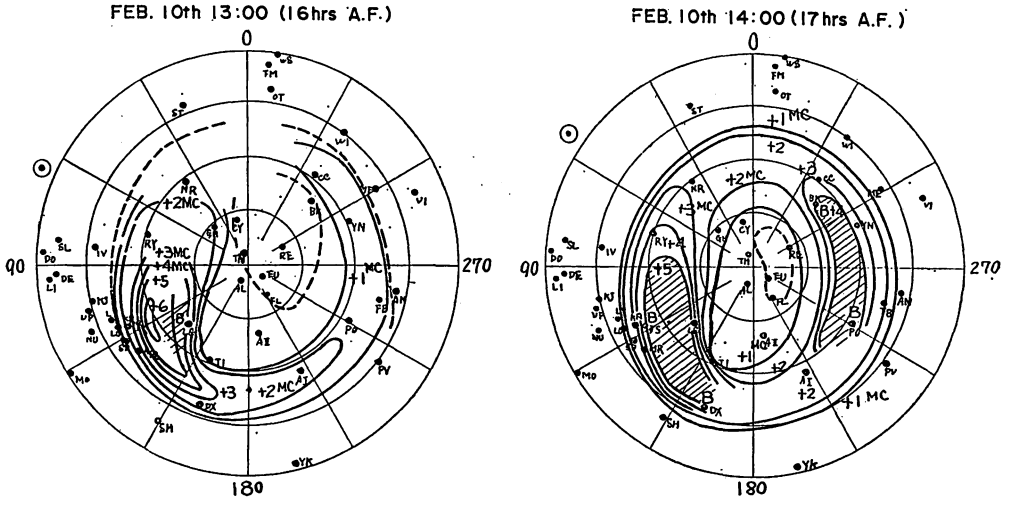

Fig. 5-4. Development of $(PCA)_A$ (northern g.m. coordinates).

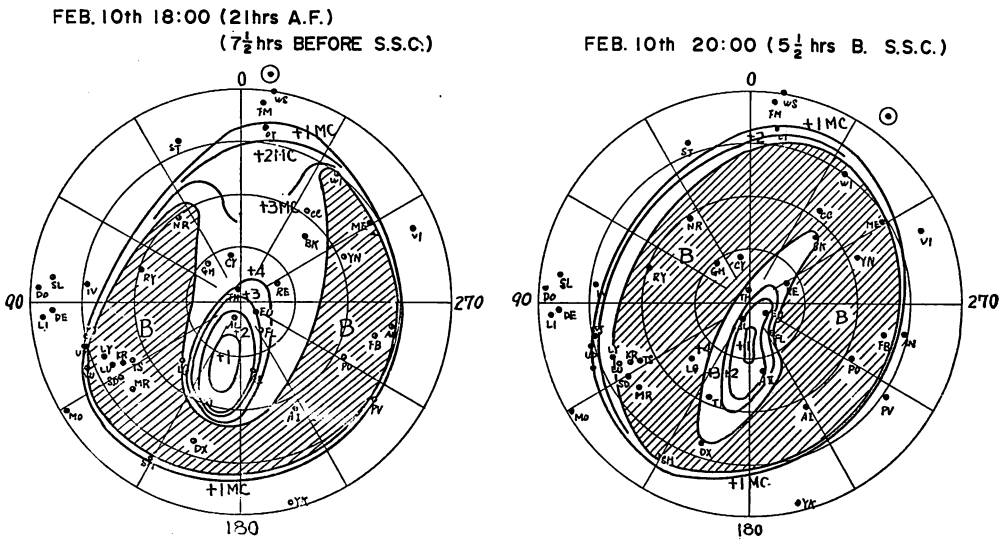

Fig. 5-5. Development of PCBO (northern g.m. coordinates).

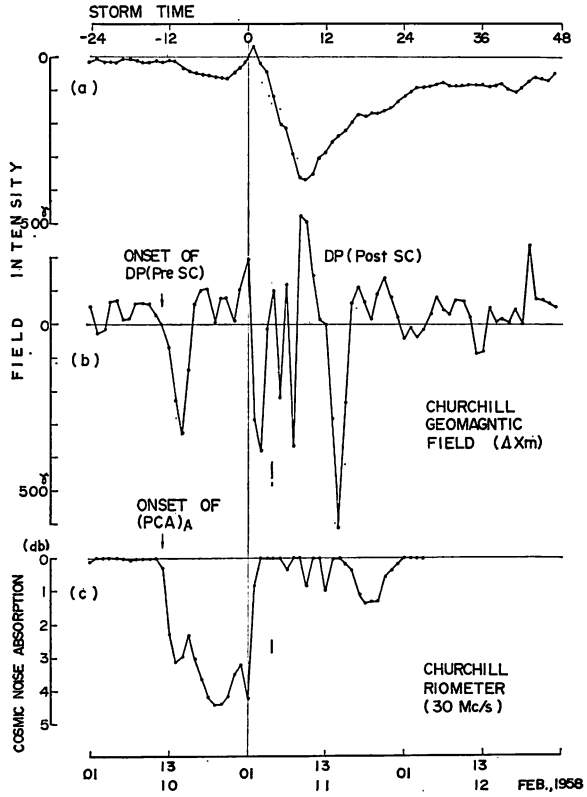

Fig. 8. Storm-time variations of Dst (32.5°), ΔX_m (Churchill), and cosmic noise absorption at Churchill (D. H. Jelly, 1961).

its long duration and smooth variation, the (PCA)A can never be identified as the auroral zone absorption in zig-zag shape which usually appears after the onset of s.s.c. The DP (PreSC) might be a special disturbance whose origin was connected with the invasion of PCA-producing solar cosmic rays into the polar ionosphere.

Several authors including Leinbach (1962) and Obayashi (1962) discussed a complex case of successive major flare events where the solar cosmic rays produced by the second flare underwent remarkable modulation by the foregoing magnetic gas cloud which existed between the sun and the earth. The magnetized cloud would trap the solar cosmic rays and sweep them out at its attainment to the earth, causing a sharp increase of PCA.

The simultaneous occurrence of (PCA)A and DP(PreSC) in the present events has some resemblance to the complex case mentioned above. As an alternative model with the one shown in Fig. 6, we could assume a foregoing weak cloud which could act as a magnetic barrier for the sub-solar cosmic rays and store a majority of them in a space between the barrier and a shock formed in front of advancing plasma cloud (Fig. 9-(1)). Some leakage of solar cosmic rays from the barrier might be responsible for a slightly enhanced ionization (PCA)p, as shown in Fig. 9-(2), while (PCA)A would be produced by a bulk of solar cosmic rays stored behind the barrier (Fig. 9-(3)).

However, the last model requires some singular mode of magnetic barrier which must be transparent for the ordinary cosmic rays, since there is no Forbush decrease of cosmic ray intensity at the time of (PCA)A. It should also be noticed that the present Pre-SC geomagnetic storm, DP (Pre SC), is a peculiar phenomenon predominating just in the polar region, with little Dst component. Table 2 gives the ratio of $|\overline{\Delta X_m}|_{max}$ to $|D_{st}^{32.5}|$ at both Pre-SC and Post-SC stage of the storm on Feb. 11. $|D_{st}^{32.5}|_{max}$ means the maximal value of $D_{st}^{32.5}$ shown in Fig. 8, while $|\overline{\Delta X_m}|_{max}$ is the mean value of $|\overline{\Delta X_m}|_{max}$ observed at 9 high-latitude stations, i.e. College, Sitka, Dixon, Tiksy, Lerwick, Tromsö, Dombås, Lovö, and Rudskov.

The ratio $|\overline{\Delta X_m}|_{max}/|D_{st}^{32.5}|_{max}$ at Pre-SC is about 3 times higher than at Post-SC, telling that the DP(PreSC) was a peculiar type of polar disturbance with little Dst component. Since Dst is produced by the corpuscular cloud rushing on to the earth, the present result seems to place on unreasonable requirement on the model shown in Fig. 9.

Table 2.
Magnitudes of D$_{st}$-components of Pre-SC and Post-SC disturbance

Disturbance \ Stage	Pre-SC	Post-SC	Ratio $\frac{\text{Post-SC}}{\text{Pre-SC}}$
$\lvert\overline{\Delta X_m}\rvert_{max}$	272 γ	611 γ	2.25
$\lvert D_{st}^{32.5}\rvert_{max}$	$<60\,\gamma$	350 γ	<5.83
Ratio $\frac{\lvert\overline{\Delta X_m}\rvert_{max}}{\lvert D_{st}^{32.5}\rvert_{max}}$	>4.53	1.75	

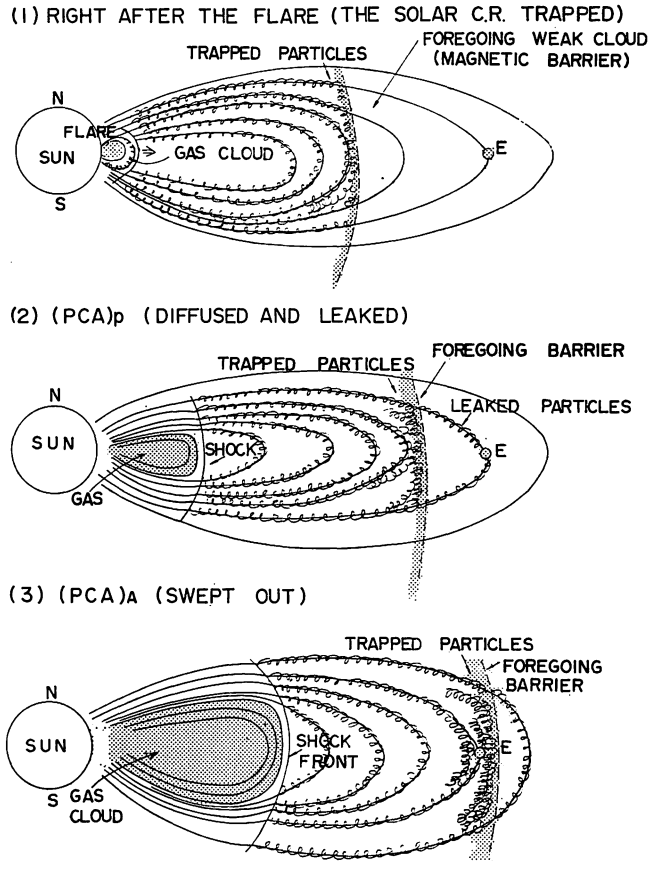

Fig. 9. Pictorial representations of a hypothetical mechanism which might explain the two-stepped occurrence of (PCA)p and (PCA)A.

3.3. Unusual increase of ionization right before the SC1- (PCA) preSC1

Axford and Reid (1962, 1963) found a remarkable enhancement in the intensity of polar cap absorption before the SC1 of the geomagnetic storm on February 11; the enhancement is seen at stage γ of riometer traces of Fort Yukon, Alaska and Churchill, Canada, in Fig. 7-(b') and (b''). The universal time change of absorption ($\overline{\Delta f_{min}}$) in the polar region also shows the pre-SC enhancement of PCA ((PCA)preSC1 in Fig. 7-(a)).

They interpreted the effect in terms of compression of the particles between two shockwaves in the interplanetary madium. One of these shock waves is formed in front of the advancing solar gas cloud and propagates through the interplanetary space supersonically and produces the sudden commencement of a geomagnetic storm at its attainment to the earth, whereas the other is a standing shockwave set up by the motion of the solar wind past the earth's magnetosphere. During a similar event on September 30, 1961, the equipment on board the satellite Explorer XII and Injun I confirmed their prediction that the enhanced absorption is due to

an increase in the low-energy protons whose energy is less than 100 MeV.

In the present sub-section, the latitudinal extent of the pre-SC enhancement will be discussed in some detail, since we have far more ionospheric sounding records than the riometer observations used in the former research. Fortunately,

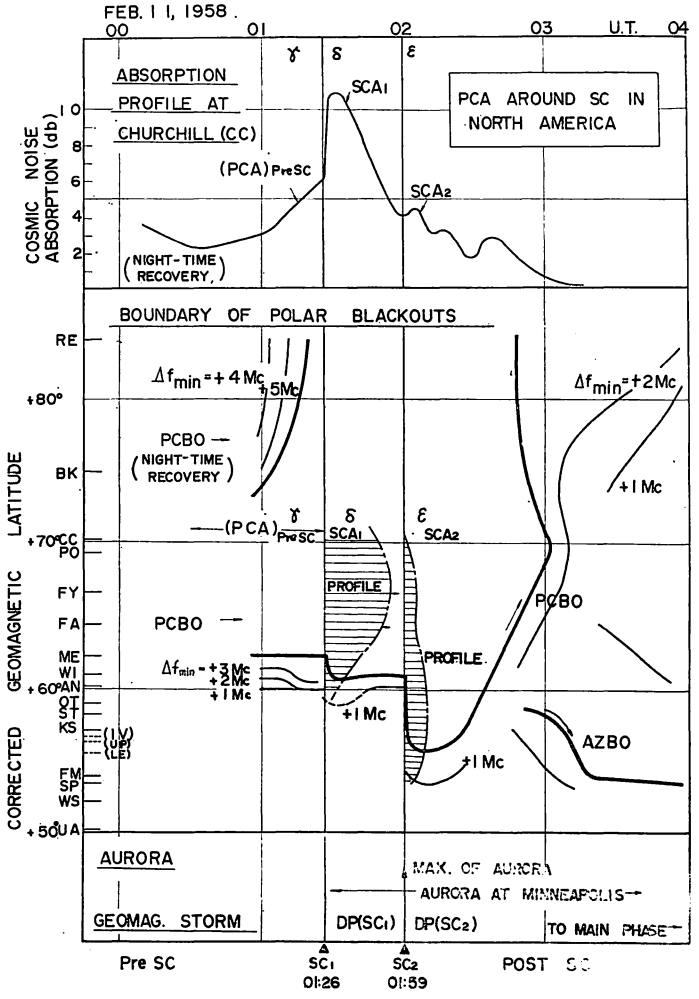

Fig. 10. Outstanding changes of PCA around the 2-stepped sudden commencements of Feb. 11, 1958 (Successive occurrence of (PCA)pre-SC1, SCA1, SCA2, and deformed PCBO).

Absorption profile at Churchill: Cosmic noise absorption observed by riometer at 30.0 Mc/s (after Axford and Reid, 1962).

Boundary of polar blackouts: Thick lines show the boundary of complete blackouts, while thin lines are contours of iso Δf_{min}. Ionization profiles at SC1 and SC2 are obtained by the standarized Δf_{min} and cosmic noise absorptions at 19 stations.

Aurora: Observation at Mineapolis at 56.8 corr. g.m. lat. (after Winckler, et al., 1959).

some of f_{min} values in the North American region had been relieved of blackout condition right before the SC1, because of the nighttime recovery of absorption. The middle part of Fig. 10 shows the time-variation of the boundaries of PCA, obtained on the analysis of Δf_{min} and riometer records at 19 ionospheric stations. The thick lines in the figure represent the boundary of blackout region, whereas the thin lines are the iso-Δf_{min} curves in step of 1.0 Mc/s. In the upper part of the figure, the Churchill-riometer is again reproduced to show the timely change of PCA intensity inside the blackout region.

During preSC enhancement of PCA (stage γ), the upper boundary of the absorption remarkably shifted towards the northern pole, whereas the lower boundary remained almost unchanged and stayed around the latitude of Anchorage, Alaska (+60.5 corrected g.m. lat.). The pattern of WPCBO (the whole polar cap blackout) shown in Fig. 5-6-left is due to the (PCA)preSC1 around the pole. The present analysis, thus, clarified the fact that the preSC-invasion of accelerated interplanetary particles took place over the whole polar cap above 60° in corrected geomagnetic latitude. The result shows a difference from the PCA events on May 8, 1960, and September 30, 1961, where the pre-SC increase of absorptions is not evident at high-latitude stations, whereas a clear increase occurred at the auroral-zone stations, suggesting that rather broad diffused impact zone exists for the accelerated protons in the auroral-zone latitudes (Axford and Reid, 1963). However, it seems quite possible that the impact zone broadens with the increasing intensity of accelerated particles of lower energies. The pre-SC enhancement of February event was the severest among three examples discussed here. The timely change of upper boundary of PCBO at this event (Fig. 10, stage γ) actually shows the broadening of the impact zone in coincidence with the increasing absorption at Churchill riometer.

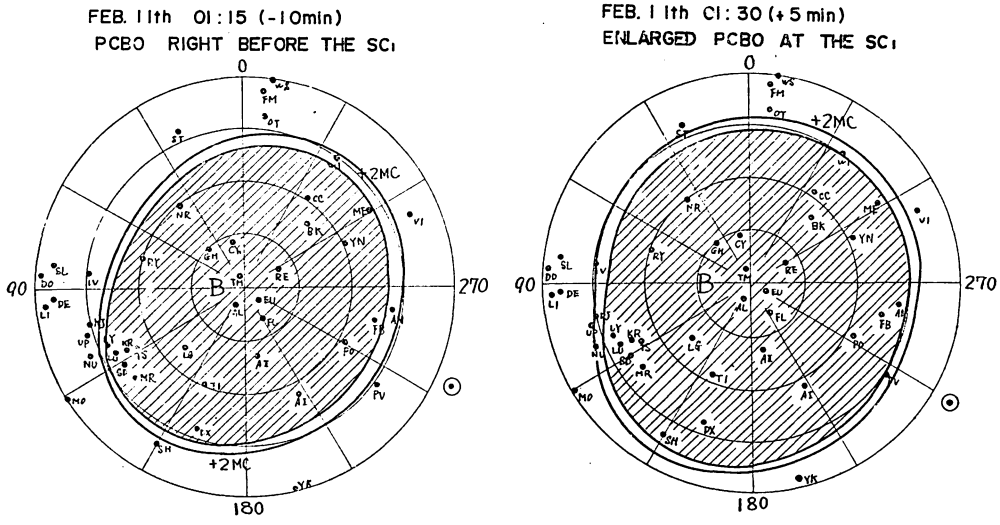

Fig. 5-6. PCBO right before and after the SC1 (01:26 on Feb. 11).

3.4. Outstanding geomagnetic and ionospheric disturbances associated with two successive sudden commencements - SCA1 and SCA2; DP (SC1) and DP (SC2)

The appearance of the earth storms associated with two successive sudden commencements on Feb. 11 was really spectacular. To understand a variety of violent terrestrial disturbances, the world-wide changes in the magnetograms are reviewed at first. In Fig. 11-(a), longitudinal variations of the geomagnetic disturbance are displayed in terms of horizontal intensities observed at four middle-latitude stations situated at equal longitudinal intervals (Kakioka, 206.1° g.m. longitude; Tucson, 312.2°; San Juan, 3.2°; Tashkent, 143.8°). The right and left columns in Fig, 11-(b) give the latitudinal changes that appeared in both the North American and the European regions, where the horizontal components of geomagnetic intensities at several stations are arranged in the order of their geomagnetic latitudes.

In all these magnetograms, two sharp increases are seen both at 01 : 26 and 01 : 59 on Feb. 11 to indicate the occurrence of successive sudden commencements of the geomagnetic storm (SC 1 and SC 2). Following the sudden commencements, violent polar geomagnetic disturbances were observed in all the magnetograms displaying remarkable diurnal variations (DP (SC 1) and DP (SC 2)). Equivalent current systems for these DP-storms are shown in Figs. 3-(7) and (8). Fukushima and Abe (1958), in their analysis of 7 Japanese magnetograms, examined the latitudinal dependence of DP (SC 1) and predicted that the disturbance must be of polar origin. The present analysis has revealed somewhat detailed appearance of two-stepped polar geomagnetic disturbances. According to the statistical study in the geomagnetic change immediately after the sudden commencement, such as by Obayashi and Jacobs (1957), the current systems as in these cases are generally observed in higher latitudes. It is interesting that the present current systems of DP (SC)'s are considerably wide-spread and cover alsmost the entire world.

In accord with the geomagnetic disturbances, the region of polar cap blackouts also showed remarkable expansions. The pattern of enhanced ionization at 01 : 30 shown in Fig. 5-6-right suggests that the first expansion occurred within at most 5 minutes after the SC 1. Detailed patterns of the boundary change have been obtained on the analysis of ionospheric data at 19 polar stations and are shown in the middle part of Fig. 10. Immediately after the SC 1, the lower boundary of the enhanced ionization suddenly shifted to the south by a few degrees of corrected geomagnetic latitude.

The profile of ionization intensity may be estimated at the analysis of the standarized cosmic noise absorptions and Δf_{min}'s. As shown by the hatched region in Fig. 10 (indicated by the letter δ), the region of increased ionization right after the SC 1 is confined within some extended auroral zone including Churchill and Anchorage. The profile may be identified with that at the SCA (Sudden Commencement Absorption) which is now widely recognized as the absorption associated with complex types of sudden commencements (Brown, et al., 1961; Ortner, et al., 1961; Matsushita, 1961). Thus the present ionization is called SCA1. The origin of sudden commencement absorption (SCA 1) is considered to be the dumping electrons from a part of Van Allen belts which were compressed by the shock wave responsible for the SC 1. Indeed, the bright aurora was visually observed

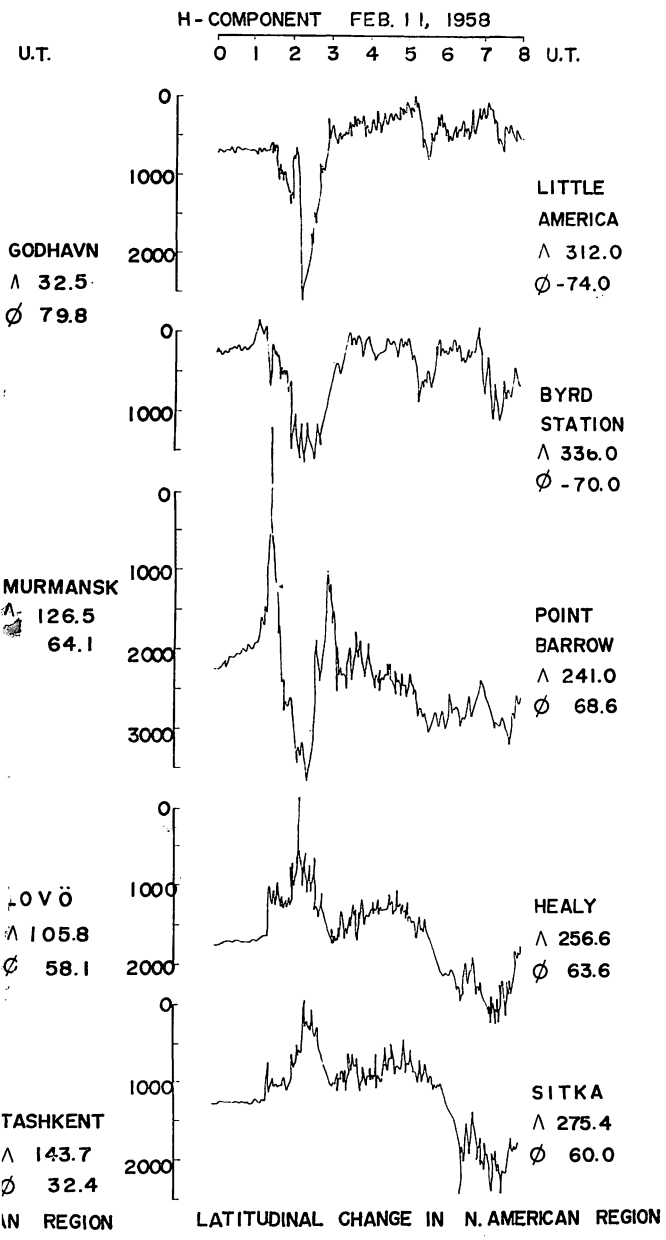

of the Feb. 11, 1958, event, expressed by the

atitudinal change in North American region.
itudinal change in European region.

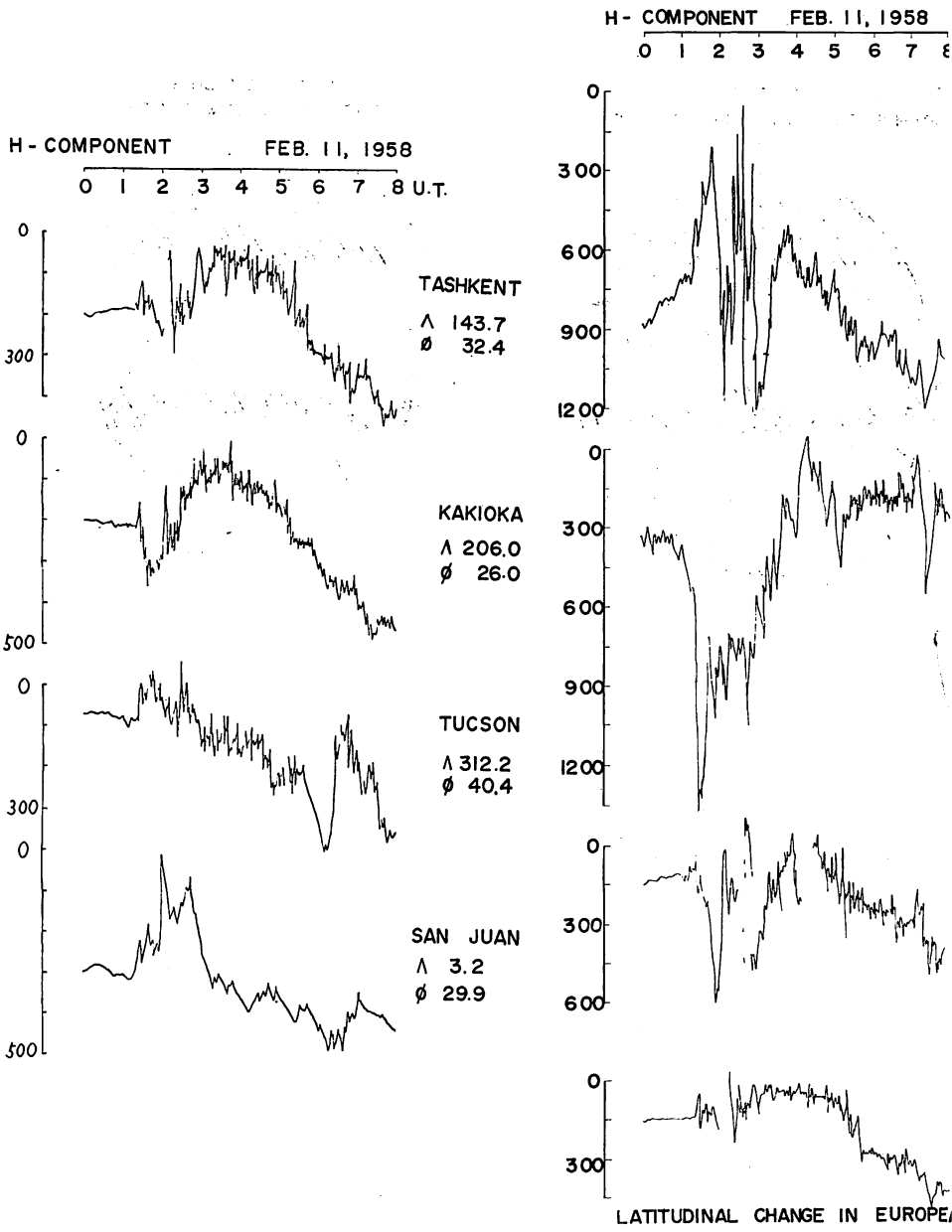

Fig. 11. Remarkable variations of geomagnetic field in the earlier part
horizontal components of various stations.

Fig. 11-(a): Local time variation in the middle latitude.

Fig. 11-(b) { Right column:
Left column:

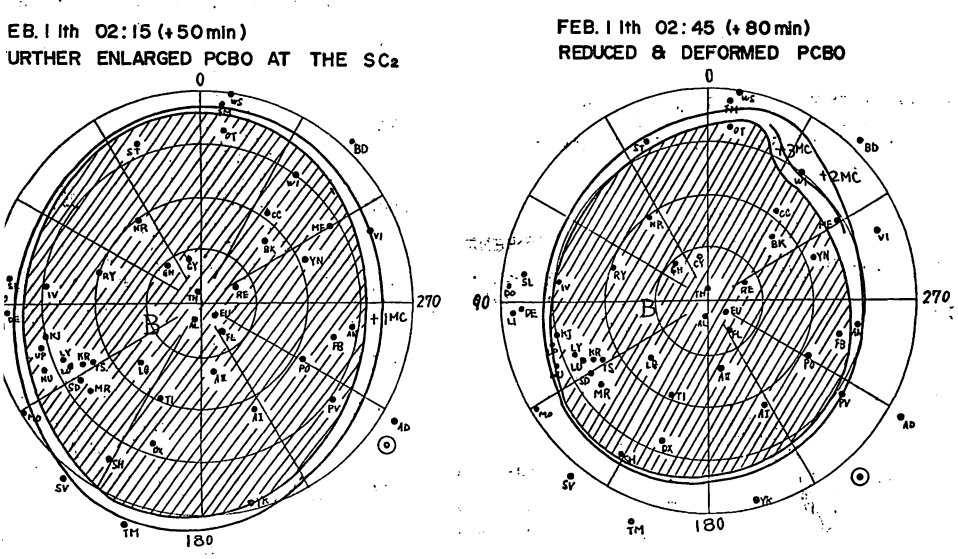

Fig. 5-7. Change of PCBO after the SC2 (01:59 on Feb. 11).

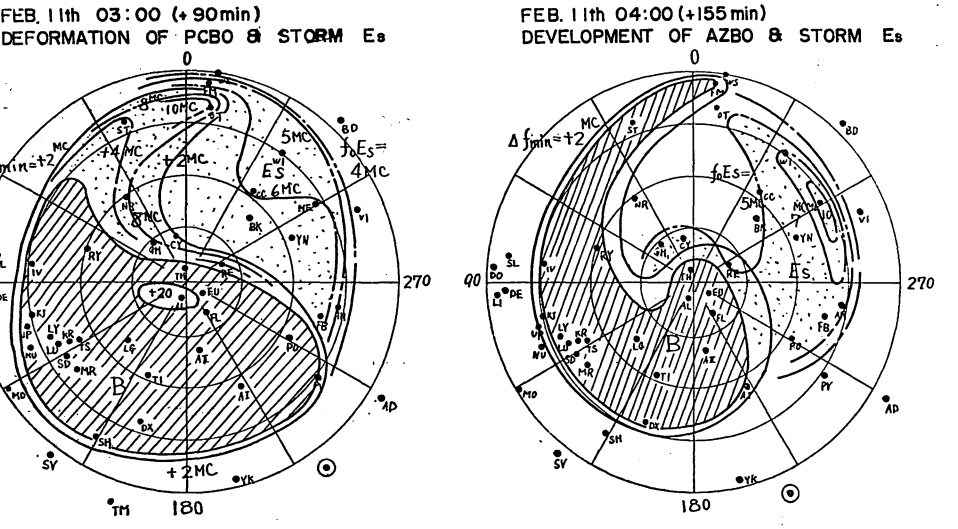

Fig. 5-8. Deformation of PCBO and development of AZBO and storm E_s (northern g.m. coordinates).

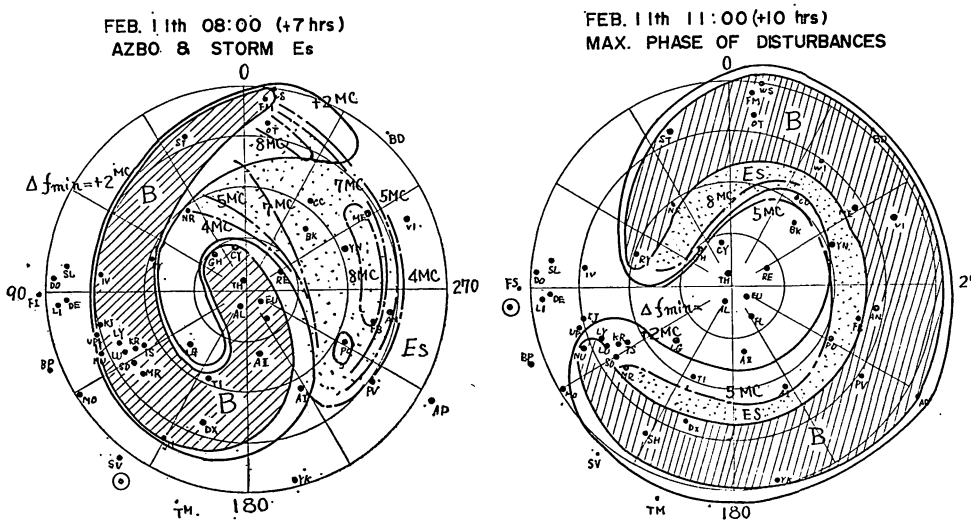

Fig. 5-9. Well-developed AZBO and storm E_s during the main phase of geomagnetic storm.

simultaneously with the SC 1 even in the subauroral zone of the North American region, showing the invasion of electron beams into the lower ionosphere (Winckler, et al., 1959).

Axford and Reid (1962) identified the enhanced absorption at this stage with the continuation of (PCA)preSC 1 which was discussed in the last subsection. It is very likely that a part of the enhanced ionization associated with SC2 was produced by the particles stored in a space between two shock-waves which were responsible for SC 1 and SC 2. Such part may be called (PCA)preSC2.

A more remarkable southward shifting of PCA boundary was observed after the SC 2, as shown in Fig. 10 (stage ε); at its maximum phase, the border of enhanced ionization attained even to Sampson, Canada. Fig. 5-7-left shows the maximum phase of the expanded PCBO region which appeared at 02: 15 U.T. on Feb. 11. The absorption profile at this stage is also given in Fig. 10; as shown by the hatched region (indicated by ε), the enhanced ionization covered the wide range between Churchill and Sampson ($+70°\sim53.6°$ in corrected geomagnetic latitudes$\equiv 8.5\ R_E\sim 2.8\ R_E$ equatorial distances of the corresponding geomagnetic field). The sudden commencement absorption (SCA2) might be connected to the second attack of shockwave to the earth whose influence reached unexpectedly inner region of Van Allen belt, squeezing out the trapped electrons into the subauroral ionosphere. It is tempting to note that the intense and dynamic aurora of higher latitude were observed even at Minneapolis ($+56.8$ c.g.m.l.) at this stage of disturbance (Winckler, et al., 1959).

Several years ago, Obayashi (1958) estimated the change of equivalent geocavity boundary size, on the analysis of the changing period of geomagnetic pulsations in the course of the present geomagnetic storm. Though the change is not of a monotonic curve as he drew, the original values show a very good coincidence

with the boundary change of PCBO shown in Fig. 10, when we transform the cavity boundary (Rc) to the geomagnetic latitude (Φ), using the formulae: $R_C = R_E \sec^2\Phi$. The result gives further support to the idea that the influence of two-stepped shock waves reached the inner region of the earth's atmorphere far beyond the ordinary cavity boundary at the time of SC's on Feb. 11, reducing the period of pulsation through their excitement of inner geomagnetic field, and squeezing out the particles stored in the region.

3.5. Remarkable deformation of PCBO region, and development of AZBO and storm E_s in the course of geomagnetic storm

Within an hour after the SC 2, the riometor record at Churchill quickly recovered to its normal value as shown in Fig. 10. Hultqvist, Aarons, and Ortner (1959) found that such kind of pronounced recovery of absorption sometimes occurred during the initial phase of PCA-assoicated magnetic storms. Further statistical study has shown that the initial phase recovery is probably restricted to the boundary of the polar cap region and localized to certain longitudes (Ortner, Leinbach, and Sugiura, 1961). However, there has been no way to prove the fact through the data of IGY riometer stations which were localized to certain longitude (Leinbach, 1962).

The present analysis of Δf_{min} data, however, has revealed the detailed patterns of deformed PCBO region in the course of the geomagnetic storm on Feb. 11, 1958. The deformation of PCBO region started soon after the maximum phase of SCA 2; at 02: 30, the boundary of PCBO began to recede to the higher latitude in the North American region as shown in Fig. 10. Further details of the degenerative polar cap blackouts can be seen the top-viewed patterns of Δf_{min}'s shown in Figs. 5–7-right and 5–8-left. At 03: 00, the recovery of absorption was already evident on the border line of the North American auroral zone, including Anchorage, Meanook, and Winnipeg. Within next 15 minutes, the blackout region underwent a remarkable shrinkage over almost the entire region in North America situated on the afternoon side, while the wide area in the Eurasian region on the morning side persisted in the blackout condition. Appearance of the wide-spread storm E_s region on the afternoon side attracts our attention.

Obayashi and Hakura (1960-a, -b) explained the temporary degeneration of polar blackouts in the initial phase of geomagnetic storm in terms of the displacement of cut-off latitude for particles, due to the compression of geomagnetic field by the advancing solar plasma. However, this explanation seems to be valid only for the average variation of cut-off latitude taken over the world-wide transition of PCBO boundary. The remarkable longitudinal change of the blackout condition mentioned above requires some additional explanations. Any modification of the cavity boundary's shape seems to be unsuitable for explanation, since the solar plasma can never make such a selective compression as it could produce a considerable recession of cut-off latitude only on the afternoon side.

Another tempting explanation was proposed by Hultqvist, et al. (1959) that the enhanced ionization might be removed by the sudden occurrence of a vertical electric field from the height region where the absorption effect is maximal. However, the interaction of the geomagnetic field with the electrojet current shown in

Figs. 3-8~9 induces a ponderomotive force in the evening side plasma so as to make it convergent and raise its ionization height. Both effects seem to be favorable for the increase of ionization in the lower ionosphere, contrary to the decreased ionization which was realized in the present event (T. Yonezawa, private communication, 1964).

A simple interpretation is the alternation of decaying PCBO with the AZBO which started in the course of the geomagnetic storm. The intensity of primary solar cosmic rays might rapidly decrease as soon as the earth is embedded in such a dense solar plasma as that at an unusually severe geomagnetic disturbance on Feb. 11, 1958.

After 04: 00, the enhanced ionization of the polar ionosphere shows the characteristic patterns where the AZBO extends itself on the morning side, embracing the region of storm E_s observed in the evening polar region, as seen in Figs. 5-8~9, or 3-10~13. These patterns of polar disturbances are quite similar to those obtained in the analysis of the Sept. 13th, 1957, events (Hakura, Nagai and Sano, 1961) and of the Nov. 6, 1957, events (Hakura and Nagai, 1964). Thus, it may safely be said that these patterns show a typical configuration of polar ionospheric disturbances.

The individual patterns discussed above show a very good coincidence with the patterns of polar blackouts and storm E_s obtained statistically by several authors (for instance, Kasuya, 1960, 1963; Kamiyama H., 1962; Thomas, 1962, etc.).

These experimental patterns of ionospheric and geomagnetic disturbances will afford useful test materials for the recent theories of the interlinkage between the magnetospheric and ionospheric disturbances, such as by Axford and Hines (1961), Piddington (1963), and Oguchi (1962).

At 10h~11h on Feb. 11, around the maximal epoch of Dst decrease of the geomagnetic storm, a spectacular equatorward shifting of the enhanced ionization region was achieved as shown in Fig. 5-9-right or Fig. 3-14. The lower boundary of blackouts and storm E_s are situated at considerably low latitude, while almost the dead calm condition is seen over the polar ionosphere above 70° in the geomagnetic latitude. The agreement is astonishing, when the pattern is compared with the large-scaled auroral strip obtained by Akasofu (1962). According to his analysis, the auroral strip lay between the curves $L=3$ and 10 (equivalent to 55°~72° in the corrected geomagnetic latitude) along the extended auroral zone in North America and Siberia at about 10: 50 on Feb. 11. It is at this maximal phase of the distusbance that the aurora was visually observed even in the middle latitude zone like Japan (Huruhata, 1958; Hikosaka, 1958). An ionospheric sounder at Kokubunji caught the auroral-type echoes with rapid fading (Nakata, 1958). Meanwhile, a sharp rise of the fading rate appeared in the JJY signal of H. F. standard frequency waves as measured at Hiraiso (Hakura and Takenoshita, 1958), showing the occurrence of radio aurora unfamiliar at such low-latitude stations as in Tokyo, Japan.

The remarkable equatorward shifting of the auroral zone during the main phase of a geomagnetic storm is explained mostly by the decrease of geomagnetic cut-off for incoming particles owing to the inverse field set up against the geomagnetic field (Obayashi and Hakura, 1960-a; Kellog and Winckler, 1961: Akasofu, Lin, and Van Allen, 1963). In addition to this, the effect of the local magnetic field due to the auroral zone current must be taken into account, as suggested by

Vestine and Sibley (1960). The westward electrojet tends to cause the lowering of the mirror point for invading particles in the southern part of the jet. Thus, the westward current situated over Alaska in Fig. 3-14 might have contributed to the tremendous equatorward shifting of auroral-zone conditions obrerved in the Pacific area.

3.6. Two characteristic phases of $F2$-layer storm - D1($F2$) and D2($F2$)

As already mentioned, the contour maps of percentage deviations of $F2$-layer critical frequencies (f_0*$F2$) shown in Figs. 3-6~16 display the progressive patterns of $F2$-layer storms in the northern hemisphere. In the course of geomagnetic disturbance on Feb. 11, 1958, the $F2$-layer storm appeared in two characteristic phases which are called D1($F2$) and D2($F2$).

In order to describe the details of these storm phases, we shall divide the $F2$-layer disturbance (D($F2$)) into two parts, storm-time variation (Dst($F2$)) and disturbance daily variaton (Ds($F2$)), following the former works of $F2$-layer storms such as by Martyn (1953), Sinno (1954), Obayashi (1959), Nagata (1954), and Matsushita (1959). Fig. 12-A shows the Dst-variation of f_0*$F2$ (Dst(f_0*$F2$)) in the northern hemisphere (lower figure), in comparison with that of the geomagnetic storm (upper figure) during Feb. 10-12, 1958. The convenient method used here in obtaining the Dst's is explained in Appendix II.

Some complicated patterns of Dst(f_0*$F2$) may become understandable, when compared with those of Sept. 12-14, 1957 events shown in Fig. 12-B. As already discussed elsewhere (Hakura, Nagai, and Sano, 1961), the latter event gives one of typical examples of $F2$-layer storm, though its magnitude is again ranked in the top class among the disturbances observed during the last period of high sunspot activity. At this event, the deterioration of f_0*$F2$ started several hours after the onset of geomagnetic storm from around the auroral zone. As the deterioration was intensified in the course of storm time, the region of $F2$-layer continued to expand till it covered almost the entire world several hours after the maximal phase of the associated geomagnetic storm.

In contrast to the September 1957 event, Dst (f_0*$F2$) shows quite an uncommon feature of disturbance in the initial phase of the February, 1958 event; soon after the onset of the associated geomagnetic storm, the entire world suddenly underwent a tremendous depression of $F2$ layer critical frequency. The mean percentage depression (f_0*$F2$) was over 40 at its maximum. Since the occurreuce of the world-wide $F2$ layer storm is quite unusual in such an early stage of disturbance, the depression (D1($F2$)) is distinguished from the second $F2$ layer storm (D2($F2$)) which started at 06: 00 on Feb. 11. The latter is one of the usual type of $F2$-layer storm, since its progress pattern is entirely identical to those in September 1957, except some difference in magnitude and duration.

In the present subsection, we would not develop the general theory of $F2$-layer storms. Our interest here is concentrated in the patterns and origin of this special type of $F2$-layer storm.

Figs. 13 and 14 display somewhat detailed characteristics of D($F2$) in terms of storm time(Dst)- and local time(Ds)- variations of f_0*$F2$ and h'*$F2$ in +20° zone where the vertical sounding records are absolutely safe from the blackout condition. Here, h'*$F2$ means the percentage deviation of $F2$ layer virtual height ($h'F2$),

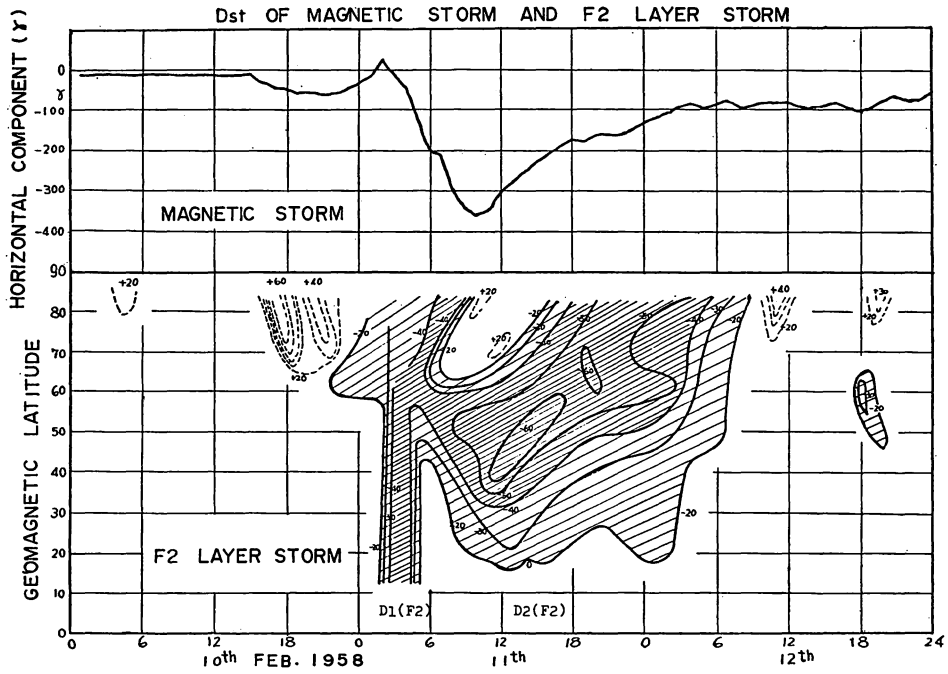

Fig. 12-(A) Dst-parts of geomagnetic storm (upper) and percentage deviation of f_0F2 (lower) on Feb. 10-12, 1958. In the lower figure, 2-stepped occurrence of $F2$-layer storm is clearly seen (D1($F2$) and D2($F2$)).

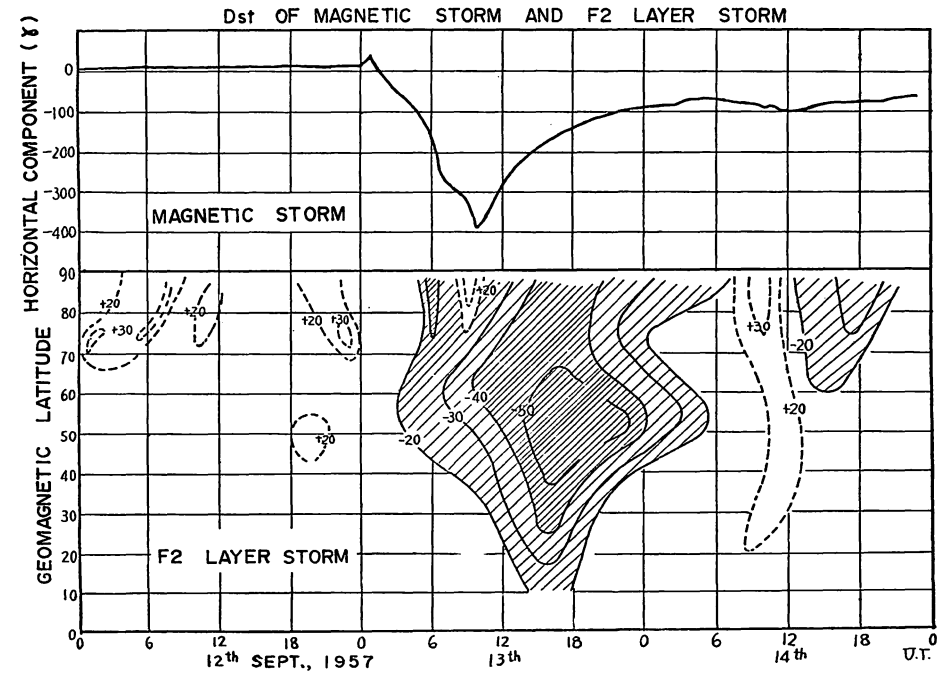

Fig. 12-(B) Dst-parts of geomagnetic storm (upper) and percentage deviation of deviation of f_0F2 (lower) on Sept. 12-14, 1957.

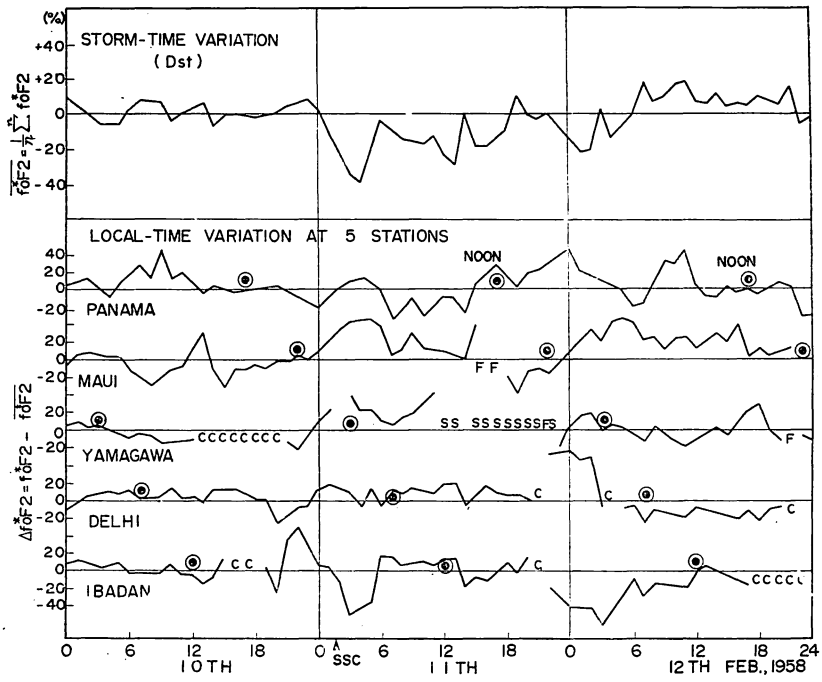

Fig. 13. Storm-time and local-time variations of f_0*F2 in the low-latitude zone (Zone VI in Table A-II).

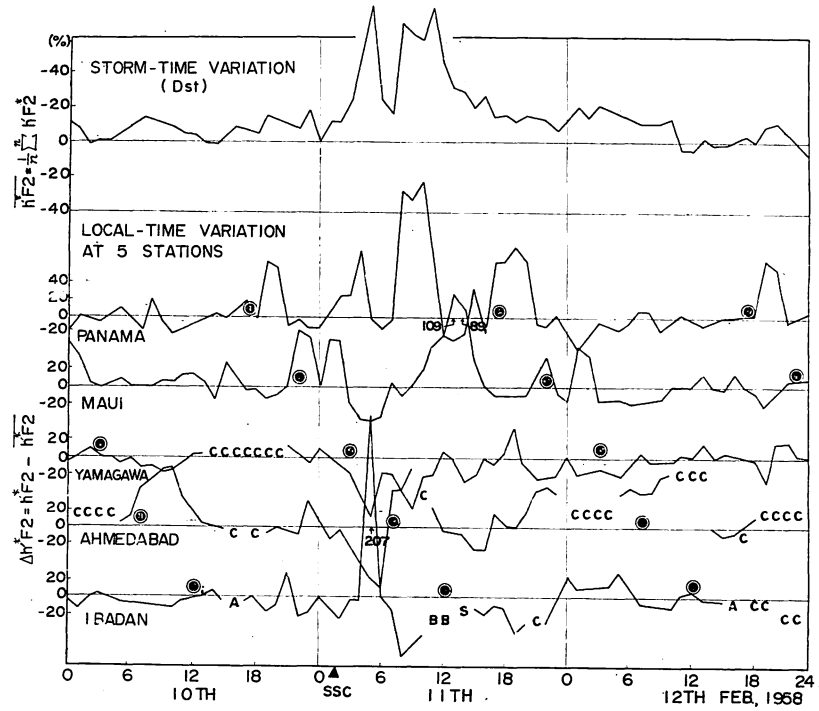

Fig. 14. Storm-time and local-time variations of $h'*F2$ in the low-latitude zone (Zone VI).

and the method of obtaining its Dst-and-Ds variations is explained in Appendix II. In the analysis of local time variations, the stations, Panama, Maui, Yamagawa, Delhi (or Ahmedabad), and Ibadan, are selected to represent the variations at equally spaced longitudes. The local noon at each station is indicated by the solar sign ⊙.

As shown at the top of the figures, the storm-time change of D1 ($F2$) is characterized by the sharp and short-lived depression of critical frequency (f_0F2) and the simultaneous increase of $F2$ layer virtual height ($h'F2$) right after the onset of geomagnetic storm (indicated by the wedge-shaped sign ▲). In addition to the Dst-variation, there is a remarkable local time variation in D1 ($F2$). At the stations on the afternoon side, i.e. at Panama and Maui in Fig. 13, Ds-variation of $f_0{}^*F2$ show a plus-ward deviation, whereas the situation is reversed at the forenoon side station, i.e. at Ibadan. There is no appreciable change at the local noon stations such as at Yamagawa and Delhi, indicating that an unusual depression of f_0F2 observed in the Asian region is mainly composed of Dst part of D1 ($F2$). The Ds-variations of $h'{}^*F2$ in Fig. 14 show a tendency nearly inverse to those of f_0F2. These characteristics of Ds-variation of D1($F2$) coincide well with those of the normal $F2$ layer storms obtained by the former researchers on their statistical analysis of a number of $F2$ layer storms at individual stations (for example, Martyn, 1953; Sinno, 1954; Matsushita, 1959; Sato, 1956, 1957).

Matuura (1963) studied the vertical structure of the F-region in the D1 ($F2$) of the Feb. 11 event by the use of $N(h)$ profiles above Kokubunji. A theoretical examination led him to a conclusion that the temperature rise due to heating by HM waves during the disturbed period was the main cause of the F region disturbance. Actually, the deteriorated electron density of the F-layer can be reasonably understood in terms of heating of the upper atmosphere which brings about enhancement of chemical reactions there (Yonezawa, 1962). Of course, it must be noted that Matuura's experimental material is restricted in the Dst part of a peculiar type of disturbance as described in the present analysis, and thus some additional examination is necessary for the discussion of the $F2$-layer storm in general. It is tempting, however, to figure that the violent pulsations on a world-wide scale seen in the initial phase of the geomagnetic storm on Feb. 11 might be induced by a successive attack of shock waves on the earth's magnetosphere. Successive invasions of the HM waves raised the temperature of the ionosphere to the higher and higher value which produced the severest expansion of the $F2$ layer as observed during the initial phase of the Feb. 11 events.

In Fig. 15 showing the time variation of electron density at Kokubunji on Feb. 11, 1958, a minor but clear depression of electron density was detected right after the second sudden commencement (SC2), prior to the large depression of electron density in the D1 ($F2$) stage (02 : 30～05 : 00). An integration of such minor depression might compose the severe decrease of electron density in the latter case. It reminds us of a clear frequency change of F-layer propagating waves at the time of a sudden commencement which was detected by Doppler technique (Davies, Watts and Zacharisen, 1962). The decreased frequency usually lasts several minutes after the sudden commencement, suggesting an expansion of the $F2$ layer due to the invading HM wave. Further statistical and theoretical

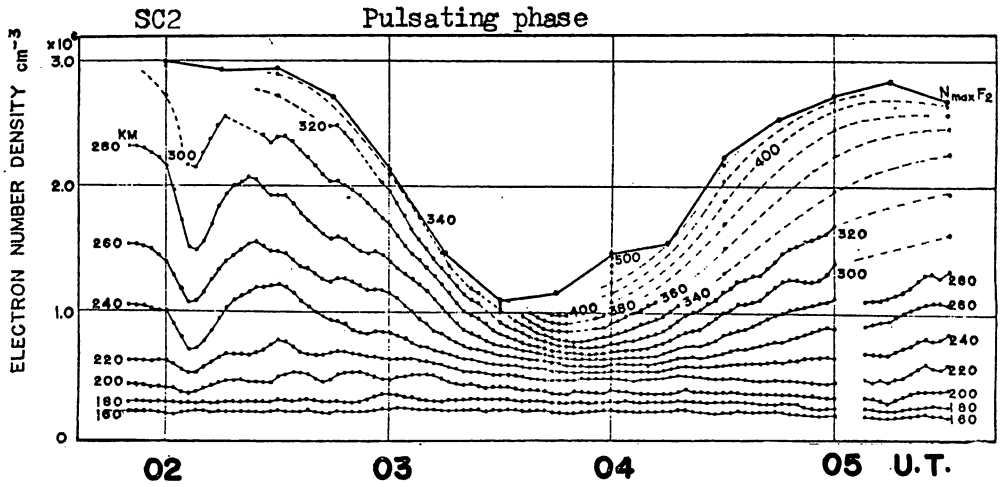

Fig. 15. Time variation of electron density at Kokubunji on Feb. 11, 1958 (Matuura, 1963).

examination are needed in this aspect, though, of course, the $F2$ layer in general has too complicated features to accept such a simple geophysical standpoint.

In the present subsection, the morphology of peculiar type of $F2$ layer disturbance in the initial phase of the Feb. 11, 1958 event was discussed by the use of the ionospheric sounding data in the northern hemisphere. More comprehensive patterns of f_0F2 in this disturbance are made by Mr. K. Sawada, member of the Radio Research Laboratories, on the world map of geographical coordinates. His results are displayed in Appendix IV with some modifications.

4. Conclusions

In the present paper, comprehensive studies were made of severe solar-terrestrial disturbances on Feb. 9–12, 1958. The important experimental results obtained here are described with some speculations as follows:

(1) A solar event responsible for a series of terrestrial disturbances is identified as a major flare that appeared at the centre of the solar disk at 21: 08 UT on Feb. 9, accompanied by an outstanding outburst of type IV.

(2) After considerably long delay of 8 hours, a polar cap absorption ((PCA)p) started in some restricted area near the geomagnetic poles, showing the first impact of solar cosmic rays into the earth's ionosphere. The progressive pattern of (PCA) p was fairly systematic. The long delay is understood in terms of the entrapment of solar cosmic rays in the magnetized plasma cloud and the diffusion process of released particles through the ambient interplanetary magnetic field. The location of the first impact zone suggests the importance of a neutral point of geomagnetic field formed on the intersurface of the cavity for the invasion of solar cosmic rays into the earth's atmosphere.

(3) After 7 more hours, a sudden development of PCA started in the sunlit

auroral zone. The enhanced ionization ((PCA)$_A$) encircled the whole auroral zone within an hour or two, and then developed gradually till the blackout condition was attained over the whole polar cap right before the sudden commencements at 01 : 26 on Feb. 11. The patterns of PCA seem to describe the formation and growth of the impact zone for the high energetic particles which were, after their release from the entrapment in the solar cloud, directly channeled to the interplanetary magnetic field lines connected to the earth.

A geomagnetic disturbance DP(PreSC) was observed over the polar region, simultaneously with the occurrence of (PCA)$_A$, far preceding the s.s.c. on Feb. 11. Because of the absence of usual Dst-part, the DP(PreSC) is considered to be a special disturbance whose origin is connected with the invasion of PCA-producing solar cosmic rays into the polar ionosphere.

(4) An unusual increase of ionization occurred right before the onset of the s. s. c. over the whole polar cap ((PCA)preSC). Axford-Reid model (1963) of 2 shockfronts acceleration of interplanetary particles may be accepted as its origin. Some progressive pattern of the impact zone for the particles was obtained in the analysis of a number of ionospheric data. The upper boundary remarkably shifted towards the geomagnetic pole with the increasing flux density of energetic particles, while the lower boundary remained almost unchanged at the latitude of about 60° throughout the course of the event.

(5) Soon after the two successive sudden commencements at 01 : 26 and 01 : 59 on Feb. 11 (SC1 and SC2), violent geomagnetic disturbances of polar origin appeared in all the magnetograms over the world (DP(SC1) and DP(SC 2)). In accord with the geomagnetic disturbances, the region of polar cap blackouts also showed two-stepped expansions. By the use of corrected geomagnetic coordinates, the transcient boundary changes in blackout region and the ionization profiles were clarified in their details. Consequently, the additional two-stepped ionizations were identified with a kind of the sudden commencement absorptions (SCA1 and SCA2). The origin of SCA's is considered to be the dumping electrons squeezed out from Van Allen belt by the influence of advancing shock waves responsible for the SC's. The speculation is supported by the simultaneous appearance of violent aurora in the sub-auroral zone.

Changes of geo-cavity boundary estimated by Obayashi (1958) on the analysis of geomagnetic pulsation periods show a nice coincidence with the boundary changes of PCBO obtained here.

(6) Soon after the SCA 2, the region of PCBO underwent a remarkable deformation. In a half hour, the blackout condition completely disappeared on the afternoon side of the polar cap, while, on the morning side, the region of blackout showed a gradual extension towards the lower latitude. A possible explanation for this is the transition to the AZBO from the decaying PCBO due to the exhaustion of solar cosmic rays inside the dense solar plasma which already attained to the earth. The AZBO is produced by the interaction of the advancing solar plasma with the earth's upper atmosphere.

(7) During the main phase of the geomagnetic storm, the enhanced ionization of the polar ionosphere showed a typical disturbance pattern. The region of AZBO extended itself on the morning side, embracing the storm E_s which appeared on the evening side of the polar region.

In its maximal phase, a spectacular equatorward shifting of the enhanced ionization region was achieved, in nice agreement with the extension of the auroral strip drawn by Akasofu (1962). At this stage, geophysical conditions in the usual subauroral zone were conveyed well south to the minauroral region, including Japan.

(8) In the course of the geomagnetic disturbance, $F2$-layer storm appeared in two characteristic phases. One (D1 ($F2$)) was an absolutely uncommon type of storm, where the entire world suddenly underwent a tremendous depression of $F2$-layer critical frequency soon after the onset of the associated geomagnetic storm, while the other (D2 ($F2$)) was considered to be the normal $F2$-layer storm which usually occurred in the main phase of a geomagnetic storm.

The Dst-part of D1 ($F2$) is characterized by the sharp and short-lived depression of critical frequency with the simultaneous increase of $F2$-layer virtual height, in the pulsating phase of the geomagnetic storm. The expansion of the $F2$ layer is understood in terms of heating of the upper atmosphere due to the successive invasion of HM waves which produced giant pulsations in the magnetograms all over the world.

Acknowledgments

In concluding, the authors wish to express their thanks to Dr. T. Yonezawa, the Radio Research Laboratories, for his discussions and interest in the present study.

The author's cordial thanks are due to Prof. T. Obayashi of Kyoto University, to Dr. Sínno, Hiraiso Radio Wave Observatory, the Radio Research Laboratories, and to Dr. K. Yanagihara, Kakioka Magnetic Observatory, for their valuable discussions bestowed on the subject.

The author are also grateful to Dr. H. Uyeda, Director of the Radio Research Laboratories, and to Dr. T. Yoshimatsu, Director of Kakioka Magnetic Observatory, for their interest in the present study.

References

Akasofu, S.-I. and S. Chapman, Large-scale auroral motions and polar magnetic disturbances-III. The aurora and magnetic storm of 11 February 1958, J. A. T. P., **24**, 785 (1962).

Akasofu, S.-I., W. C. Lin and J. A. Van Allen, The anomalous entry of low rigidity solar cosmic rays into the geomagnetic field, J. G. R., **68**, 5327 (1963).

Axford, W. I. and C. O. Hines, A unifying theory of high latitude geophysical phenomena and geomagnetic storms, Can. J. Phys., **39**, 1433 (1961).

Axford, W. I. and G. C. Reid, polar cap absorption and the magnetic storm of Feb. 11 1958, J. G. R., **67**, 1962 (1962).

Axford, W. I. and G. C. Reid, Increases in intensity of solar cosmic rays before sudden commencements of geomagnetic storms, J. G. R., **68**, 1793 (1963).

Blokh, Ya. L., L. I. Dorman, and N. S. Kaminer, The effect of intensity-increase of cosmic radiation prior to magnetic storms, Cosmic Ray Conf., Moscow, English edition, **4**, 173 (1959).

Brown, R. R., T. R. Hartz, B. Landmark, H. Leinbach, and J. Ortner, Large-scaled electron bombardment of the atmosphere at the suudden commencement of a geomagnetic storm, J. G. R., **66**, 1035 (1961).

Chapman S. and M. Sugiura, A study of the morphology of magnetic storm, Sci. Rep. Geophysical Inst. Alaska Univ. (1959).

Davies, K., J. M. Watts, and D. H. Zacharisen, A study of *F*2-layer effects as observed with a Doppler technique, J. G. R., **67**, 601 (1962).

Fukushima, N. and S. Abe, The initial phase of the magnetic storm on Feb. 11, 1958, Rep. Ionos. Res. Japan, **12**, 44 (1958).

Hakura, Y. and Y. Takenoshita, On the short wave transmission disturbance of Feb. 11, 1958, Rep. Ionos. Res. Japan, **12**, 10 (1958).

Hakura, Y., Y. Takenoshita and T. Otsuki, Polar blackouts associated with severe geomagnetic storm on Sept. 13, 1957 and Feb. 11, 1958, Rep. Ionos. Res. Japan, **12**, 459 (1958).

Hakura, Y. and T. Goh, Pre-SC polar cap ionospheric blackout and type IV solar radio outburst, J. Radio Res. Lab,, **6**. 635 (1959).

Hakura, Y., Development of ionospheric and geomagnetic storms caused by solar corpuscular emissions-I. polar cap blackout and auroral zone blackout, Rep. Ionos. Space Res. Japan, **15**, 1 (1961-a).

Hakura, Y., M. Nagai and Y. Sano, Development of ionospheric and geomagnetic storms caused by solar corpuscular emissions-II. Polar blackouts, storm Es, and geomagnetic storms, Rep. Ionos. Space Res. Japan, **15**, 14 (1961).

Hakura, Y., Some statistics on the solar cosmic rays produced by solar eruptions associated with type IV outbursts, Proc. 12th Alaskan Sci. Conf. (1961-b).

Hakura, Y., Patterns of polar cap blackout drawn in a geomagnetic coordinate corrected for the higher terms of spherical harmonic development, J. Radio Res. Lab., **11**. No. 57, to be published (1964).

Hakura, Y. and M. Nagai, Spatial extent of polar enhanced ionization during geomagnetic bay disturbance (to be published).

Hikosaka, T., On the great enhancement of the line [OI] 6300 in the aurora at Niigata on Feb. 11, 1958, Rep. Ionos. Res. Japan, **12**, 469 (1958).

Hultqvist, B., The geomagnetic field lines in higher approximation, Arkiv Geophys., **3**, 63 (1958).

Hultqvist, B., J. Aarons, and J. Ortner, Effects of the solar flare of July 7 1958 observed at Kiruna Geophysical Observatory, Sweden, Tellus, **11**, 319 (1959).

Huruhata, M., Aurora and airglow observations on Feb. 11, 1958, Rep. Ionos. Res. Japan, **12**, 40 (1958).

Kamiyama, H., The spiral ionization of the sporadic *E* ionization in the polar region, Rep. Ionos. Space Res. Japan, **16**, 415 (1962).

Kasuya, I., Statistical study in the occurrence of polar blackouts, J. Radio Res. Lab., **7**, 451 (1960).

Kasuya, I., The spiral patterns of the polar ionospheric disturbance, J. Radio Res. Lab., **10**, 177, (1963).

Kellog, P. J. and J. R. Winckler, Cosmic ray evidence for a ring current, J. G. R., **66**, 3991 (1961).

Kondo, I., K. Nagashima, S. Yoshida, and M. Wada, World-wide increase of cosmic-ray intensity associated with cosmic-ray storm, Moscow conf. (1959).

Leinbach, H., Interpretation of the time variations of polar cap absorption associated with solar cosmic ray bombardment, Sci. Rep. Univ. Alaska, UAG-R 127 (1962).

Martyn, D. F., The morphology of the ionospheric variation assoicated with magnetic disturbances, Proc. Roy. Soc. A., **218**, 1 (1953).

Matsushita, S., A study of the morphology of ionospheric storms, J. G. R., **64**, 305 (1959).
Matsushita, S., Increase of ionization associated with geomagnetic sudden commencements, J. G. R., **66**, 3958 (1961).
Matuura, N., Thermal effect on the ionospheric *F* region disturbance, J. Radio Res. Lab., **10**, 1, (1963).
Murakami, K. and S. Kudo, The onset times of cosmic-ray storms, Sci. Paper Inst. Phys. Chem. Res., **54**, 155 (1960).
Nagai, M., On the magnetic storm on February 11, 1958, Memo. Kakioka Mag. Obs., **2**, 39 (1964).
Nagata T., Ionospheric storms in high latitudes, Rep. Ionos. Res. Japan, **8**, 39 (1954).
Nakata Y., Auroral echoes in the ionograms obtained in minauroral region, Rep. Ionos. Res. Japan, **12**, 1 (1958).
Obayashi, T. and J. A. Jacobs, Sudden commencements of geomagnetic storms and atmospheric dynamo action, J. G. R., **62**, 589 (1957).
Obayashi, T., Geomagnetic storms and earth's outer atmosphere, Rep. Ionos. Res. Japan, **12**, 301 (1958).
Obayashi, T., Geomagnetic storms and ionospheric disturbances, J. Radio Res. Lab., **6**, 373 (1959).
Obayashi, T. and Y. Hakura, Enhanced ionization in the polar ionosphere caused by solar corpuscular emissions, Rep. Ionos. Space Res. Japan, **14**, 1 (1960-a).
Obayashi, T and Y. Hakura, Solar corpuscular radiation and polar ionospheric disturbances, J. G. R., **65**, 3131 (1960-b).
Obayashi, T. and Y. Hakura, Propagation of solar cosmic rays through interplanetary magnetic field, J. G. R., **65**, 3143 (1960-c).
Obayashi, T., Propagation of solar corpuscules and interplanetary magnetic fields, **67**, 1717 (1962).
Oguchi, T., Inter-relations along the outer atmosphere disturbance phenomena in the auroral zone-II, Spiral pattern of the polar aeronomical disturbances, Rep. Ionos. Space Res. Japan, **16**, 363 (1963).
Ortner, J., H. Leinbach and M. Sugiura, The geomagnetic storm effect on polar cap absorption, Arkiv. Geophys., **3**, 429 (1961).
Ortner, J., B. Hultqvist, R. R. Brown, T. R. Hartz, O. Holt, B. Landmark, J. L. Hook and H. Leinbach, Cosmic noise absorption accompanying geomagnetic storm sudden commencements, J. G. R. **67**, 4169, (1962).
Piddington, J. H., Theories of the geomagnetic storm main phase, Planet. Space Sci., **11**, 1277 (1963).
Sakurai, K., Motion of low-energy solar cosmic ray particles in the earth's magnetic field, J. G. G., **12**, 59 (1961).
Sato, T., Disturbances in the ionosheric *F*2 region associated with geomagnetic storms, I, II, and III., J. G. G., **8**, 129 (1956); **9**, 1 and 94 (1957).
Sato, T., Morphology of the ionospheric *F*2 disturbances in the polar region, Rep. Ionos. Space Res. Japan, **13**, 91 (1959).
Sinno, K., On the characteristics of *F*2-layer variations assoicated with geomagnetic storms, Rep. Ionos. Res. Japan, **8**, 28 (1954).
Sinno, K., On the great solar flare which started at 21h 09m February 9th, 1958, as the likely source of geomagnetic storm, February 11th, Rep. Ionos. Res. Japan, **12**, 6, (1958).
Sinno, K., Some characteristics on solar corpuscular radiations which excite abnormal ionization in the polar upper atmosphere, J. Radio Res. Lab. Japan, **8**, 17 (1961).
Somayajulu, Y. V., Changes in the *F*-region during magnetic storms, J. G. R., **68**, 1899 (1963).
Spreiter, J. R. and B. R. Briggs, Theoretical determination of the form of the boundary

of the solar corpuscular stream produced by interaction with the geomagnetic dipole field of the earth, J. G. R., **67**, 37 (1962).
Thomas, L., The distribution of dense E_s ionization at high latitudes, J. A. T. P., **24**, 643 (1962).
Vestine, E. H. and W. L. Sibley, The geomagnetic field in space, ring currents, and auroral isochasms, J. G. R., **65**, 1967 (1960).
Winckler, J. R., L. Peterson, R. Hoffman and R. Arnoldy, Auroral X-rays, cosmic rays, and related phenomena during the storm of Feb. 10-11, 1958, J. G. R., **64** 597 (1959).
Yonezawa, T., The characteristic behaviour of the $F2$ layer during severe magnetic storms, Proc. Int. Conf. on Ionosphere, London, 128 (1962).

APPENDIX I Data used in present paper

(i) Ionospheric sounding data

In the present analysis we used the vertical ionospheric sounding data at 126 stations (89 in the northern and 37 in the southern hemisphere), whose names, abbreviations and locations are listed in Table A-I-1. In order to represent the world-wide patterns of ionospheric disturbances, the following four elements of ionospheric sounding data are used:

Table A-I-1. Ionospheric sounding stations

Ionospheric station	Abbr.	Geomagnetic Lat.	Geomagnetic Long.	Corr. Geomagnetic Lat.	Corr. Geomagnetic Long.
Thule, Greenland	TH	88.1	1.1	(86.2)	(25.6)
Eureka, Canda	EU	86.5	236.0	88.8	252.1
Alert, Canada	AL	85.0	168.5	86.1	132.7
Fletchers Ice, Canada (drifting)	FL	(83.6)	(222.0)	(86.1)	(224.0)
Resolute Bay, Canada	RE	83.0	289.4	84.2	303.2
Clyde River, Canada	CY	81.9	0.5	81.2	16.3
Godhavn, Greenland	GH	79.8	32.7	77.8	42.4
Arctica II, USSR (drifting)	AII	(77.0)	(190.0)	(80.4)	(186.1)
Longyearbyen, Norway	LG	74.4	131.0	74.6	115.1
Baker Lake, Canada	BK	73.7	315.2	75.0	318.7
Tikhaya Bay, USSR	TI	71.5	153.2	74.3	140.3
Narsarssuak, Greeland	NR	71.2	37.6	69.3	44.6
Reykjavik, Iceland	RY	70.1	71.1	66.6	70.6
Yellowknife, Canada	YN	69.0	293.3	69.8	293.1
Churchill, Canada	CC	68.7	322.8	70.2	324.4
Point Barrow, USA	PO	68.5	241.2	69.4	246.2
Arctica I, USSR (drifting)	AI	(68.0)	(209.0)	(71.2)	(214.3)
Tromsö, Norway	TS	66.9	116.2	66.0	104.5
Kiruna, Sweden	KR	65.3	115.6	64.4	104.3
Fairbanks, USA	FA	64.6	256.6	64.6	259.4
Murmansk, USSR	MR	64.1	126.4	64.6	114.1
Sodankylä, Finland	SD	63.8	120.1	63.5	108.4

Ionospheric station	Abbr.	Geomagnetic Lat.	Geomagnetic Long.	Corr. Geomagnetic Lat.	Corr. Geomagnetic Long.
Dixon Is., USSR	DX	63.0	161.5	67.9	154.0
Luleå, Sweden	LU	62.9	114.7	61.9	104.0
Lycksele, Sweden	LY	62.5	110.8	61.0	100.7
Meanook, Canada	ME	61.8	300.7	62.3	299.4
Anchorage, USA	AN	60.9	258.2	60.5	260.4
Inverness, UK	IV	60.7	83.4	56.9	80.1
Kjeller, Norway	KJ	60.0	100.2	57.3	92.6
Providenie Bay, USSR	PV	59.7	235.6	60.3	240.7
Winnipeg, Canada	WI	59.6	322.7	61.0	321.9
Upsala, Sweden	UP	58.5	106.0	56.5	97.4
St. John's, Newfoundland	ST	58.4	21.4	58.5	28.7
Nurmijärvi, Finland	NU	57.8	112.6	56.7	104.0
Ottawa, Canada	OT	56.9	351.5	59.1	354.4
Salekhard, USSR	SH	56.4	148.5	60.8	139.4
Juliusrüh, Germany	JU	54.5	98.6	51.4	92.0
Slough, UK	SL	54.3	84.1	50.1	81.0
Victoria, Canada	VI	54.3	293.4	53.9	291.9
De Bilt, Netherlands	DE	53.7	89.5	49.7	85.0
Lindau, Germany	LI	52.1	93.9	48.4	88.6
Dourbes, Belgium	DO	51.9	87.6	47.7	83.8
Fort Monmouth, USA	FM	51.7	353.9	54.0	356.2
Yakutsk, USSR	YK	51.0	193.8	56.4	198.1
Moscow, USSR	MO	50.8	120.6	50.9	111.1
Washington, USA	WS	50.0	350.3	52.3	351.6
Poitiers, France	PS	49.5	81.8	44.7	79.5
Sverdlovsk, USSR	SV	48.5	140.7	52.2	132.1
Freiburg, Germany	FI	48.4	90.0	43.9	85.8
Schwarzenburg, Suisse	SW	48.0	88.7	43.4	84.9
Adak, USA	AD	47.2	240.1	46.7	241.8
Graz, Austria	GZ	46.9	97.0	43.1	91.5
Budapest, Hungary	BP	46.6	100.6	43.2	94.4

Ionospheric station	Abbs.	Geomagnetic Lat.	Geomagnetic Long.	Corr. Geomagnetic Lat.	Corr. Geomagnetic Long.
Tomsk, USSR	TM	45.9	159.6	52.3	155.0
Monte Capellino, Italy	MT	45.8	89.6	41.0	85.7
San Francisco, USA	SF	43.6	298.6	42.5	297.1
Rome, Italy	RO	42.5	92.0	37.6	87.9
Simferopol, USSR	SM	41.2	113.3	39.6	106.1
White Sands, USA	WH	41.0	316.4	40.4	314.4
Rabat, Morocco	RB	38.7	69.9	32.2	70.7
Grand Bahama, USA	GR	37.9	349.3	40.0	348.8
Sakhalin Is., USSR	SK	36.9	207.5	40.5	213.0
Wakkanai, Japan	WA	35.2	206.1	39.0	210.8
Alma-Ata, USSR	AA	33.5	150.8		
Ashkhabad, USSR	AS	30.6	133.5		
Akita, Japan	AK	29.4	205.5		
Tokyo, Japan	TO	25.4	205.5		
Daker, Sénégal	DK	21.8	54.6		
Maui, USA	MU	20.8	268.2		
Panama Canal Zone, Canal Zone	PN	20.6	348.6		
Yamagawa, Japan	YA	20.3	197.9		
Delhi, India	DH	18.8	149.0		
Paramaribo, Surinam	PB	17.0	15.3		
Bogota, Colombia	BG	16.0	354.5		
Okinawa, Liu Kiu	OK	15.2	195.7		
Ahmedabad, India	AH	14.1	143.8		
Taipei, Formosa	TA	14.0	189.0		
Calcutta, India	CT	12.2	158.8		
Ibadan, Nigeria	IB	10.6	74.8		
Bombay, India	BM	9.8	143.8		
Djibouti, French Somaliland	DJ	7.0	113.5		
Talara, Peru	TL	6.6	347.7		
Baguio, Philippines	BA	5.0	189.3		
Bangui, Africa France	BU	5.0	88.6		

Ionospheric station	Abbr.	Geomagnetic Lat.	Geomagnetic Long.	Corr. Geomagnetic Lat.	Corr. Geomagnetic Long.
Chiclayo, Peru	CL	4.4	349.2		
Madras, India	MA	3.3	150.3		
Chimbote, Peru	CB	2.2	350.4		
Tiruchirapalli, India	TP	1.3	148.3		
Kodaikanal, India	KD	0.7	147.5		
Trivandrum, India	TV	−0.1	146.3		
Huancayo, Peru	HU	−0.6	353.8		
La Paz, Bolivia	LP	−5.0	0.9		
Singapore, Malaya	SG	−10.0	172.7		
Hollandia, New Guinea	HL	−12.6	210.3		
São Paulo Brazil	SO	−12.9	21.0		
Tucuman, Argentine	TU	−15.3	3.3		
Tsumeb, S. Africa	TB	−18.3	82.8		
Salisbury, Phodesia	SY	−19.5	96.2		
Rarotonga, Pacific Ocean	RA	−20.9	273.8		
Buenos-Aires, Argentine	BE	−23.3	9.4		
Tananarive, Madagascar	TN	−23.7	112.6		
Concepcion, Chile	CO	−25.3	356.5		
Johannesburg, S. Africa	JO	−26.9	91.4		
Townsville, Australia	TW	−28.4	219.0		
Capetown, S. Africa	CP	−32.7	79.7		
Brisbane, Australia	BR	−35.8	226.9	−36.6	225.6
Port Stanley, Falkland Is.	PY	−40.4	9.0	−36.0	11.3
Watheroo, Australia	WT	−41.7	185.8	−42.5	184.0
Ushuaia, Argentine	US	−43.3	0.8	−39.3	5.1
Canberra, Australia	CN	−43.8	223.7	−45.2	222.0
Godley Head, New Zealand	GD	−48.1	252.8	−50.8	253.0
Deception, Antarctica	DC	−51.6	6.1	−47.4	10.6
Hobart, Australia	HB	−51.7	224.6	−53.9	222.6
Port Lockroy, Antarctica	PL	−53.4	3.9	−49.3	9.2
Kerguelen, Indian Ocean	KG	−57.2	128.0	−57.8	122.5

Ionospheric station	Abbr.	Geomagnetic Lat.	Geomagnetic Long.	Corr. Geomagnetic Lat.	Corr. Geomagnetic Long.
Campbell Is., New Zealand	CM	−57.4	253.1	−60.7	254.2
Macquarie Is., Southern Ocean	MQ	−61.1	243.1	−64.6	243.0
Halley Bay, Antarctica	HY	−65.8	24.3	−61.2	27.9
Ellsworth, Antarctica	EL	−66.9	14.7	−62.4	21.0
Byrd Station, Antarctica	BY	−70.6	336.1	−69.0	351.9
Mawson, Antarctica	MW	−73.1	103.0	−70.4	92.0
Little America, Antarctica	LA	−74.0	312.0	−74.4	332.3
Cape Hallet, Antarctica	CH	−74.6	278.1	−77.9	294.1
Terre Adelie, Antarctica	TE	−75.3	233.4	−80.1	226.8
Wilkes, Antarctica	WL	−77.9	178.8	−79.6	155.1
Scott Base, Antarctica	SC	−79.0	294.4	−80.7	323.0

(Note) For the higher latitude stations ($|\Phi_m|>35°$), the corrected geomagnetic coordinates are calculated in accordance with the Hultqvist's table (1958) which gives the displacements of the "landing points" of geomagnetic field lines, due to the four spherical harmonic terms following the dipole term (for further details, see Hakura, 1964).

f_{min} (the frequency below which no echoes are observed)

The value of f_{min} increases by the solar corpuscle bombardment on the lower ionosphere, and sometimes all ionospheric echoes are completely absorbed by unusual ionization ($f_{min}\equiv B$). Thus Δf_{min} (the deviation of f_{min} value from the monthly median) is used to analyse the polar blackouts.

$$\Delta f_{min}=f_{min}-\overline{f_{min}}$$

$\overline{f_{min}}$: monthly median of f_{min}.

The region of polar blackout is hatched in the figures.

f_oE_s (the maximum recorded frequency of sporadic E)

At high latitudes, f_oE_s increases in close association with the magnetic disturbance and visible auroral activity. They are called, for convenience, storm E_s and identified by the following criteria:

$f_oE_s\geq 5$ Mc/s (thin dot in the figures),

or $f_oE_s\geq 7$ Mc/s (dense dot).

f_oF2 (the $F2$-layer critical frequency)

For the measure of $F2$-layer storms, the percentage deviation of critical

frequency (f_o*$F2$) is used.

$$\Delta f_oF2 = f_oF2 - \overline{f_oF2}.$$

$\overline{f_oF2}$: monthly median of f_oF2.

$$f_o{}^*F2 = \Delta f_oF2 / \overline{f_oF2} \times 100\%$$

***h'F2* (the minimum virtual height of the *F2*-layer)**

The percentage deviation of vertual height is also used for the study of $F2$-layer storms.

$$h'^*F2 = \Delta h'F2 / \overline{h'F2} \times 100\%$$

(ii) Cosmic noise absorption

When the detailed profile of ionization is needed in the present analysis, the cosmic noise absorption is examined for 6 stations listed below.

Table A-I-2 Riometer Stations

Name	Abbr.	Freq.	Geomagnetic		Corrected g.m. lat.	Source
			Lat.	Long.		
Churchill	C C	30.0 Mc/s	68.7	322.8	70.2	Jelly Axford-Reid
Fort Yukon	F Y	27.6	66.7	257.1	66.7	Leinbach
Fairbarks	F A	27.6	64.6	256.6	64.6	Leinbach
Kingsalmon	K S	27.6	57.5	254.9	57.1	Leinbach
Sampson	S P	18.0	54.0	293.4	53.6	Obayashi-Jacobs
Unalaska	U A	27.6	50.9	247.9	50.0	Leinbach

(iii) Magnetic data

In order to draw the current systems, there are used the normal magnetograms and hourly values of three components of 35 magnetic stations in the northern hemisphere. The names, abbreviations and locations of those observatories are given in Table A-I-3.

Table A-I-3. Geomagnetic observatories

Observatory	Abbr.	Geomagnetic		Geographic		ϕ	$D-\phi$
		Lat. ϕ	Long. Λ	Lat. φ	Long. λ		
Thule	T h	88.0	0.0	77.5	291.0	0.0	−79.7
Resolute Bay	R e	83.0	289.0	74.7	265.5	46.5	−140.5
Godhavn	G o	79.8	32.5	69.2	306.5	−17.5	−34.8
Marchison Bay		75.2	137.2	80.0	18.3		
Baker Lake	B L	73.7	315.3	64.3	264.0		
Churchill	C h	68.7	322.7	58.8	265.9		
Point Barrow	P B	68.6	241.0	71.3	203.2	33.0	− 6.5
Tromsφ	T r	67.1	116.7	69.7	18.9	−30.8	29.7
Cape Chelyuskin	C C	65.9	117.5	77.7	104.3	− 2.3	25.4
College	C o	64.5	255.4	64.9	212.2	27.5	1.9
Big Delta	B D	64.3	259.3	64.0	214.3	26.5	3.3
Murmansk	Mm	64.1	126.5	69.0	33.0	−26.6	38.0
Healy	H e	63.6	256.6	63.9	211.1	26.2	1.8
Dickson	D i	63.0	161.5	73.5	80.4	−12.8	41.8
Lerwick	L e	62.5	88.6	60.1	358.8	−23.6	13.7
Dombås	D o	62.3	100.0	62.1	9.1	−23.6	17.6
Anchorage	A n	60.9	258.1	61.2	210.1		
Tiksy	T i	60.5	191.4	71.7	128.9	7.2	7.4
Sitka	S i	60.0	275.4	57.1	224.7	21.4	7.8
Eskdalemuir	E s	58.5	82.9	55.2	356.8	−20.4	9.7
Lovö	L o	58.1	105.8	59.4	17.8	−22.1	22.6
Rude Skov	R S	55.8	98.5	55.8	12.5	−20.6	18.1
Hartland	H a	54.6	79.0	51.0	355.5	−18.1	9.1
Yakutsk	Y a	51.0	193.8	62.0	129.7	5.8	−13.1
Fredericksburg	F r	49.6	349.9	38.2	282.6	2.6	− 9.8
Odessa	O d	43.8	111.1	46.8	30.9	−15.7	17.6
San Fernando	S F	41.0	71.3	36.5	353.8	−13.6	22.6
Tucson	T u	40.4	312.2	32.3	249.2	10.1	3.2
Tifilisi	T f	36.7	122.1	42.0	44.7	−13.1	18.3

Observatory	Abbr.	Geomagnetic		Geographic		ψ	$D-\psi$
		Lat. ϕ	Long. Λ	Lat. φ	Long. λ		
Memambetsu	M b	34.1	208.3	43.9	144.2	7.5	−15.7
San Juan	S J	29.9	3.2	18.4	293.9	− 0.7	− 6.6
Kakioka	K a	26.0	206.0	36.2	140.2	6.2	−12.6
Honolulu	H o	21.1	266.5	21.3	201.9	12.3	− 0.7
Kanoya	K y	20.7	198.1	31.4	150.9	4.2	− 9.2
Guam	G u	3.9	212.8	13.5	144.8	6.4	− 4.6

(Note) Ψ The angle formed by the great circle joining the station and the geomagnetic pole with the geographical meridian of the station (eastward positive);
D Declination (for February 1958).

APPENDIX II Method of obtaining Dst and Ds variations of f_0*$F2$, h'*$F2$ and geomagnetic storm.

Generally, the disturbance variation (D) is divided into two distinguishable parts as follows:

$$D=D_{st}+D_s,$$

where D_{st} is the storm-time variation, whereas D_s shows the local-time variation. In the present analysis, D_{st} and D_s variations of ionospheric and geomagnetic storms are discussed through the convenient presentation as follows:

(i) f_0*$F2$

(D_{st})

D_{st} (f_0*$F2$)) is defined for each of 6 zones of different latitudes in the northern hemisphere, as

$$Dst\ (f_0*F2)=\overline{f_0*F2}\,(t)=\frac{1}{n}\sum^{n}\{f_0*F2\,(t)\}\,n,$$

where suffix n shows the stations at equal longitudinal interval in each of latitude zones (**Table A–II**).

(D_s)

$\{D_s\ (f_0*F2)\}_n$ is defined for each station (n) in a latitude zone, as

$$\{Ds\,(f_0*F2)\}_n=\{f_0*F2\,(t)\}_n-\overline{f_0*F2\,(t)}=\{\Delta f_0*F2\}_n$$

(ii) h'*$F2$ ditto

(iii) Geomagnetism

(D_{st})

For a geomagnetic storm, D_{st} (X_m- or Y_m- component) at a latitude Φ is denoted

Table A-II
Zones and stations used for calculations of Dst (f_0*F2 or h'*F2) and S_D (f_0*F2 or h'*F2)

Zone I (Φ=83.8°)
Thule, Eureka, Alert, Fletchers Ice, Resolute Bay, Clyde, Godhavn.
Zone II (Φ=71.4°)
Arctic II, Longyeabyea, Baker Lake, Narsarssuak, Tikhaya, Churchill, Point Barrow, Arctic I, Reykjavik.
Zone III (Φ=61.1°)
Kiruna, Dixon, Meanook, Anchorage, Inverness, Provideniya, Winnipeg, St. Johns.
Zone IV (Φ=48.4°)
Yakutsk, Moscow, Washington, Sverdlovsk, Schwarzenburg, Adak, San Francisco.
Zone V (Φ=40.2°)
Adak, San Francisco, Rome, White Sands, Rabat, Grand Bahama, Wakkanai Ashkabad, Tomsk.
Zon VI (Φ=17.1°)
Dakar, Maui, Panama, Yamagawa, Delhi, Paramaribo, Ibadan, Djibouti.

by (D_{st}^{Φ}) X or Y. In the present analysis, $(D_{st}^{32.5})$ X and Y are obtained as the averages of both components at 6 middle-latitude stations, i.e. San Juan, San Fernando, Tifilisi, Kakioka, Honolulu, and Tucson, where S_q-variations are removed. Since the mean latitudinal distribution of D_{st} is known from Chapman and Sugiura (1959), an estimation of D_{st}^{Φ} is given by

$$D_{st}^{\Phi}=\frac{A(\Phi)}{A(32.5)}D_{st}^{32.5},$$

where $A(\Phi)$ means the relative factor of the D_{st} distribution at latitude Φ.
(D_s)

D_s (X_m- or Y_m- component) is defined for each station of latitude Φ, as

$$\Delta X_m=X_m-(D_{st}^{\Phi})\,X,$$

or

$$\Delta Y_m=Y_m-(D_{st}^{\Phi})\,Y.$$

In Fig. 3, D_s- field of geomagnetic storm is expressed by equivalent current

system, where the electric current between successive lines is 1×10^5 amps.

APPENDIX III SID effect of solar flare observed at 21: 08 on Feb. 9, 1958

SWF A small SWF was observed at Hiraiso in the field intensity of HF radio wave (WWV 15 Mc/s):

SWF (Hiraiso)

Start time	Duration	Type	Imp.
21 : 24	20 min.	slow S-SWF	1

SID (f_{min})

World-wide analysis of Δf_{min} shows that the SID effect exists inside the region ($\chi\leq80°$) even at 22: 00, as shown in **Figs. A-III-1 and -2.**

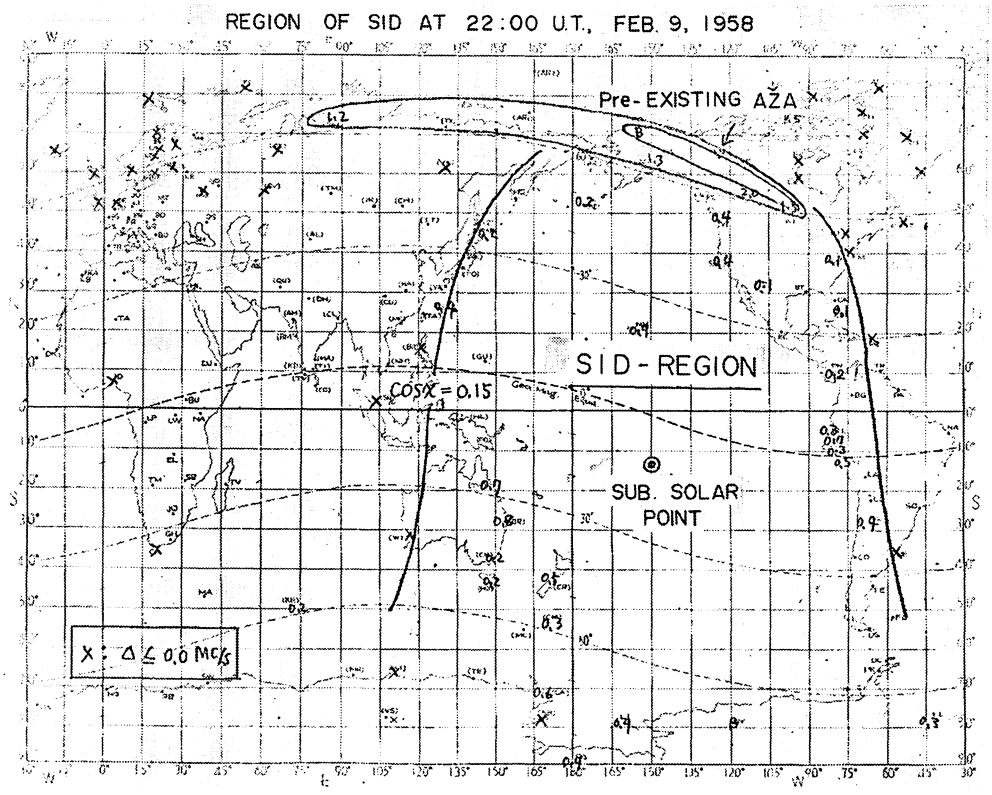

Fig. A-III-1 SID-effect at 22:00 on Feb. 9, 1958, detected by the analysis of world-wide f min values, where enchanced f min (Δfmin) is expressed as, Δf min=f min (22 h)−f min (21 h).

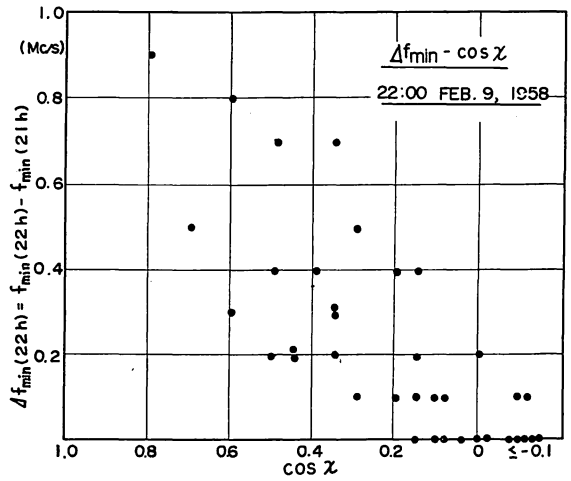

Fig. A-III-2 Δfmin vs. cos χ relation at the time of SID at 22:00 UT on Feb. 9, 1958.

APPENDIX IV Additional world charts of *F*2 layer storm (prepared by Sawada and Hakura).

As a supplement to the polar charts of *F*2 layer disturbances in Fig. 3, here we present several world-wide patterns of f_o**F*2 as given in Figs. A–IV–1∼7.

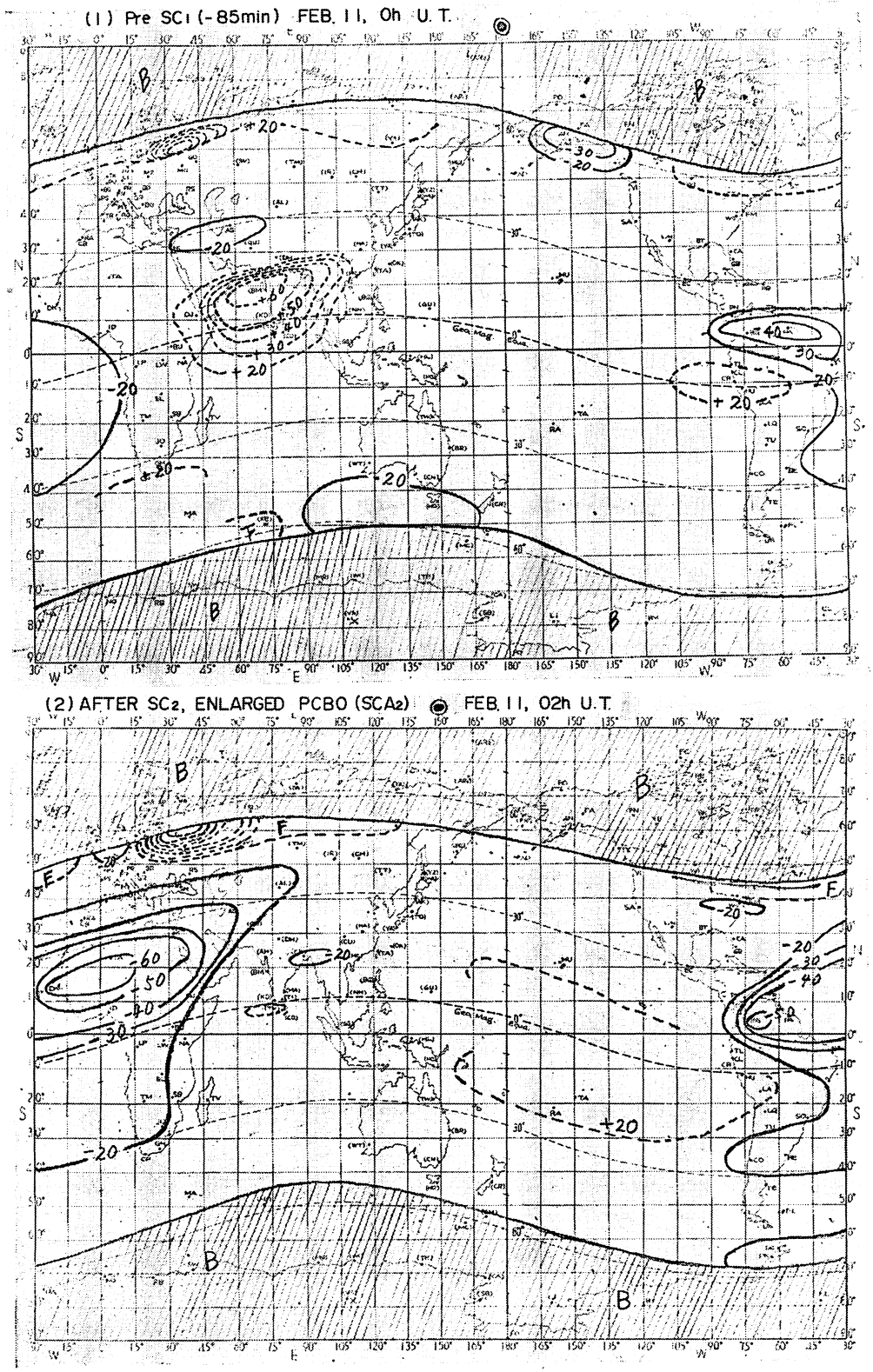

Fig. A-IV-1∼7 World maps of $F2$-layer storms on Feb. 11, 1958, expressed by the contour lines of iso-f_0*$F2$ (percentage deviation of f_0F2). In the figures, blackout regions are hatched, whereas the regions of storm E_s are dotted.

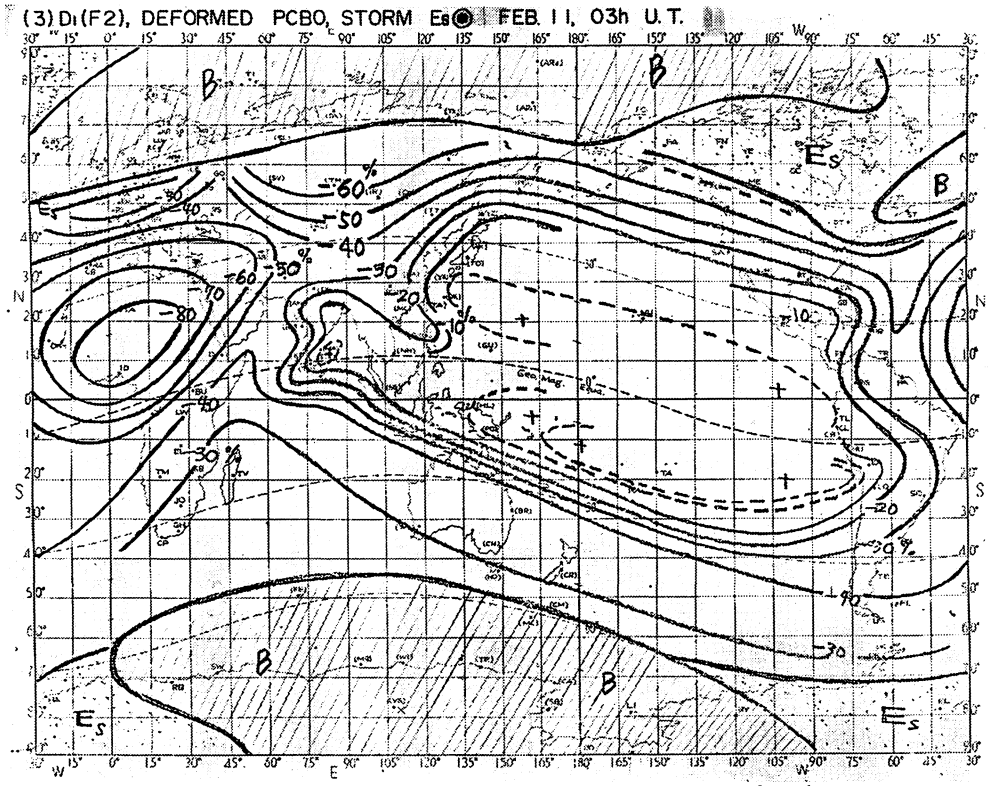
(3) Di(F2), DEFORMED PCBO, STORM Es FEB. 11, 03h U.T.
B
Es
-60
-50
-40
-30
-20
-10
+10
+20
+30
+40
+50
+60
+70
+80
+90
N
S
W
E

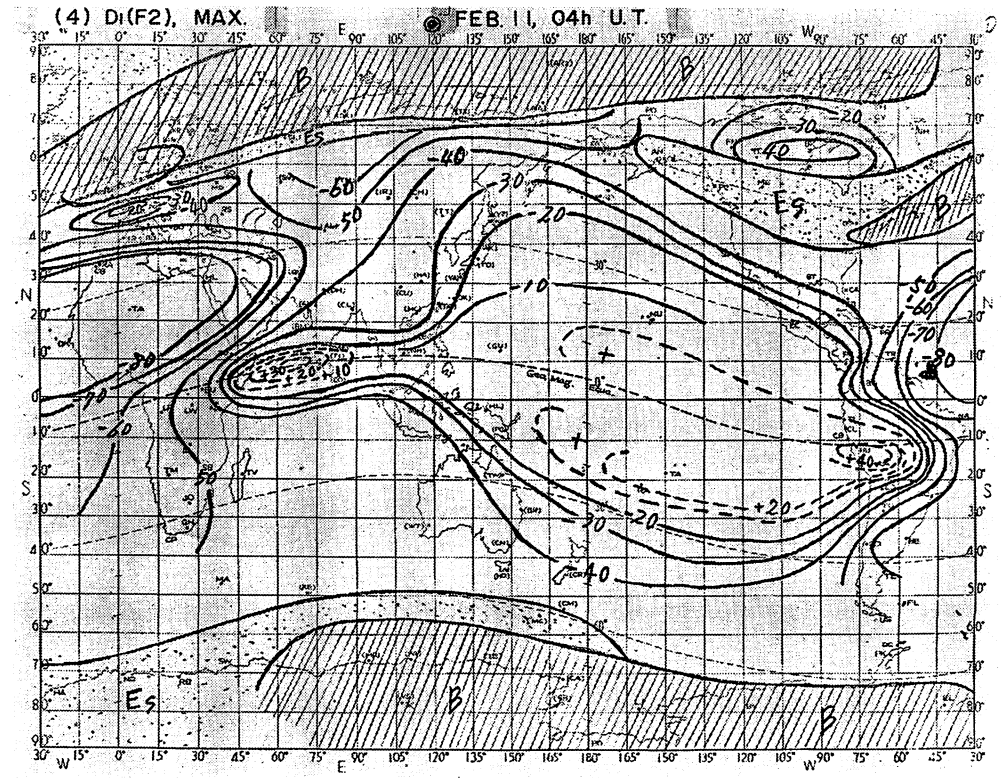
(4) Di(F2), MAX. FEB. 11, 04h U.T.
B
Es
-80
-70
-60
-50
-40
-30
-20
-10
+10
+20
+30
+40
+50
+60
+70
+80
+90
N
S
W
E

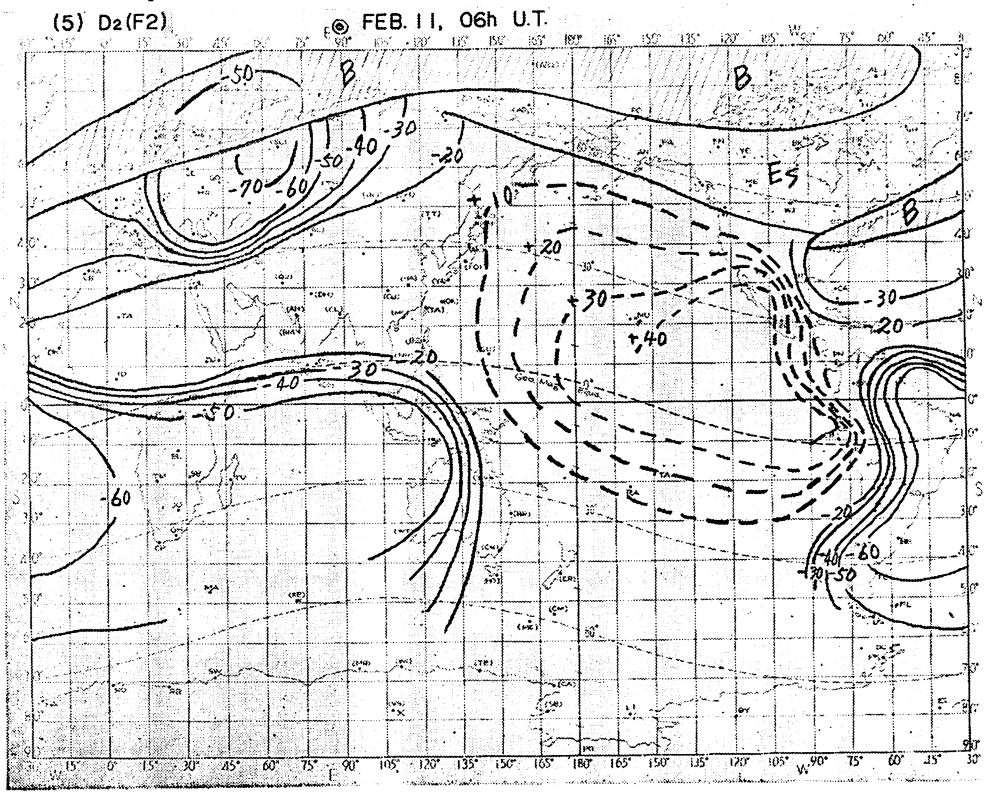
(5) D2(F2)
FEB. 11, 06h U.T.
B
B
B
Es
-50
-70
-60
-40
-30
-20
+10
+20
+30
+40
-60

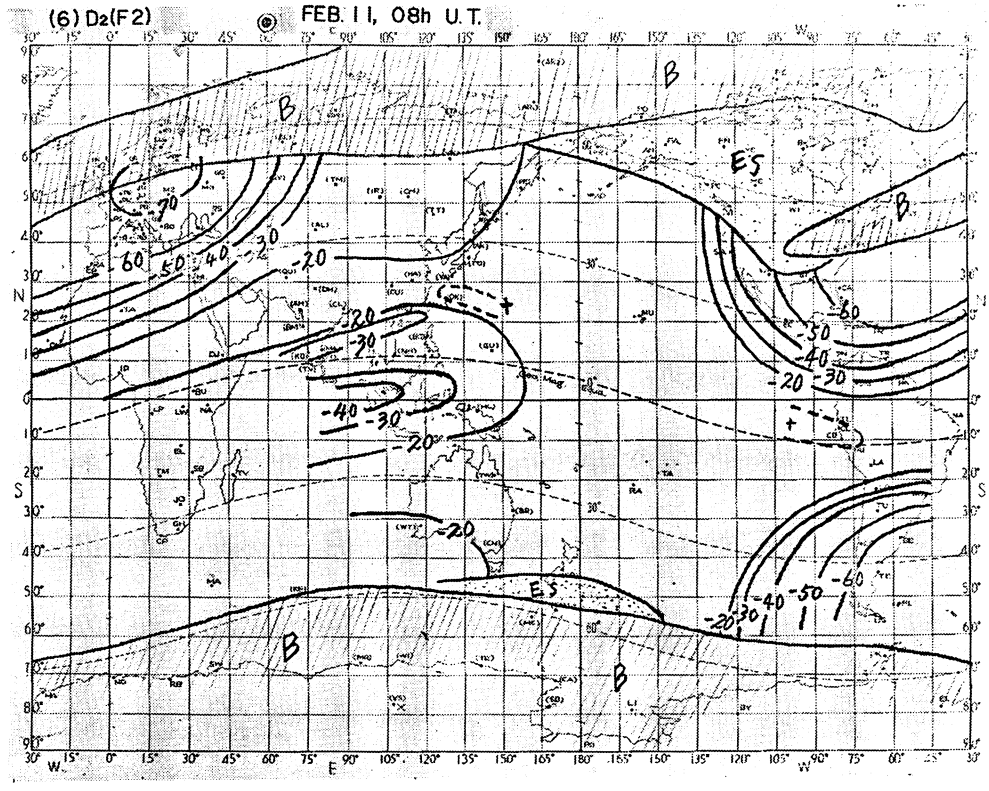
(6) D2(F2)
FEB. 11, 08h U.T.
B
B
B
Es
Es
B
-70
-60
-50
-40
-30
-20
-60
-50
-40
-30
-20

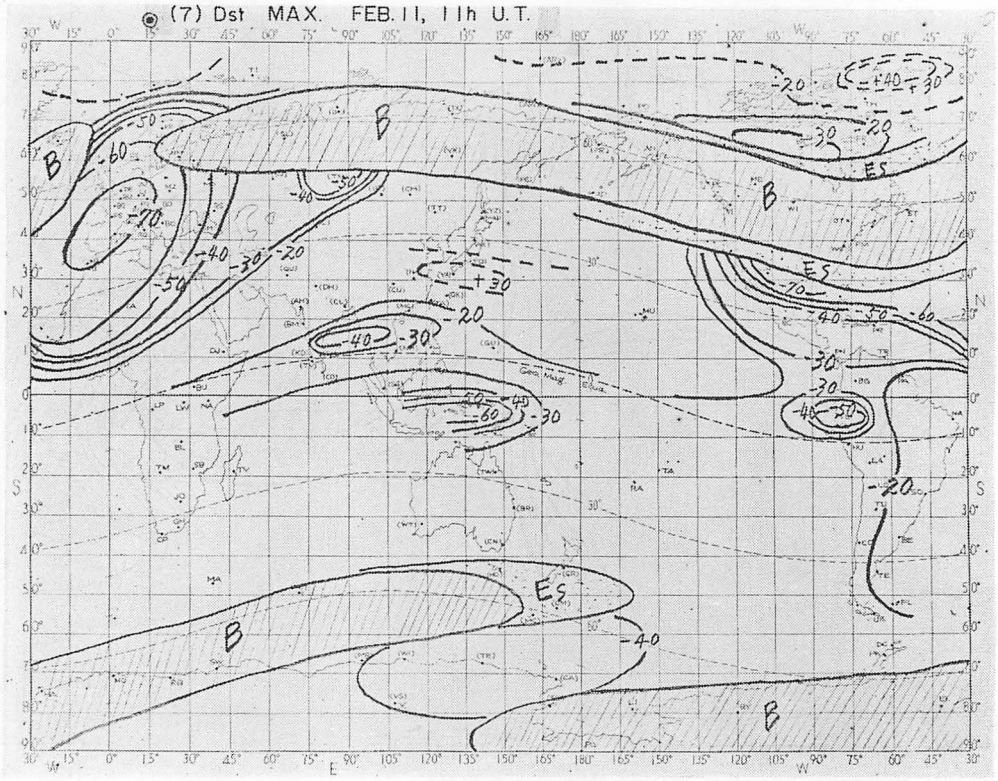
(7) Dst MAX. FEB. 11, 11h U.T.
B
Es
-20
-30
-40
-50
-60
-70
+30
+40